

1      **Nitrogen Fixation in Arctic Coastal Waters (Qeqertarsuaq, West**  
2      **Greenland): Influence of Glacial Melt on Diazotrophs, Nutrient**  
3      **Availability, and Seasonal Blooms**

4      Schlangen Isabell<sup>1</sup>, Leon-Palmero Elizabeth<sup>1,2</sup>, Moser Annabell<sup>1</sup>, Xu Peihang<sup>1</sup>, Laursen Erik<sup>1</sup>, and  
5      Löscher Carolin R.<sup>1,3</sup>

6      <sup>1</sup>Nordceee, Department of Biology, University of Southern Denmark, Campusvej 55, 5230 Odense M, Denmark

7      <sup>2</sup>Department of Geosciences, Princeton University, Princeton, New Jersey

8      <sup>3</sup>DIAS, University of Southern Denmark, Odense, Denmark

9      **Correspondence:** Carolin R. Löscher (cloescher@biology.sdu.dk)

0      **Abstract.** The Arctic Ocean is undergoing rapid transformation due to climate change, with decreasing sea ice contributing to  
1      a predicted increase in primary productivity. A critical factor determining future productivity in this region is the availability  
2      of nitrogen, a key nutrient that often limits biological growth in Arctic waters. The fixation of dinitrogen (N<sub>2</sub>) gas, a biological  
3      process mediated by diazotrophs, provides a source of new nitrogen to marine ecosystems and has been increasingly recognized  
4      as a potential contributor to nitrogen supply in the Arctic Ocean. Historically it was believed to be limited to oligotrophic  
5      tropical and subtropical oceans, Arctic N<sub>2</sub> fixation has only garnered significant attention over the past decade, leaving a  
6      gap in our understanding of its magnitude, the diazotrophic community, and potential environmental drivers. In this study, we  
7      investigated N<sub>2</sub> fixation rates and the diazotrophic community in Arctic coastal waters, using a combination of isotope labeling,  
8      genetic analyses and biogeochemical profiling, in order to explore its response to glacial meltwater, nutrient availability and  
9      its impact on primary productivity. We observed N<sub>2</sub> fixation rates ranging from 0.16 to 2.71 nmol N L<sup>-1</sup> d<sup>-1</sup>, notably higher than  
0      many previously reported rates for Arctic waters. The diazotrophic community was predominantly composed of UCYN-A. The  
1      highest N<sub>2</sub> fixation rates co-occurred with peaks in chlorophyll *a* and primary production, at a station in the Vaigat Strait, likely  
2      influenced by glacial meltwater input. On average, N<sub>2</sub> fixation contributed 1.6% of the estimated nitrogen requirement of primary  
3      production, indicating that while its role is modest, it may still represent a nitrogen source in certain conditions. These findings  
4      illustrate the potential importance of N<sub>2</sub> fixation in an environment previously not considered important for this process and  
5      provide insights into its response to the projected melting of the polar ice cover.

7      **1 Introduction**

8      Nitrogen is a key element for life and often acts as a growth-limiting factor for primary productivity (Gruber and Sarmiento,  
9      1997; Gruber, 2004; Gruber and Galloway, 2008). Despite nitrogen gas (N<sub>2</sub>) making up approximately 78% of the atmosphere,  
0      it remains inaccessible to most marine life forms. Diazotrophs, which are specialized bacteria and archaea, have the ability to  
1      convert N<sub>2</sub> into biologically available nitrogen, facilitated by the nitrogenase enzyme complex carrying out the process of  
2      biological nitrogen fixation (N<sub>2</sub> fixation) (Capone and Carpenter (1982)). Despite the fact that these organisms are highly spe-

**Deleted:** The fixation of dinitrogen (N<sub>2</sub>) gas, a biological process mediated by diazotrophs, not only supplies new nitrogen to the ecosystem but also plays a central role in shaping the biological productivity of the Arctic.

**Deleted:** Here we

**Deleted:** show

**Deleted:** to be

**Deleted:** those observed in many other oceanic regions, suggesting a previously unrecognized significance of N<sub>2</sub> fixation in these high-latitude waters.

**Deleted:** is

**Deleted:** We found

**Deleted:** ing

**Deleted:** maximum

**Deleted:** concentrations

**Deleted:** rates

**Deleted:** close impacted by glacier meltwater inflow, possibly providing otherwise limiting nutrients.

**Deleted:** Our

i4 cialized and N<sub>2</sub> fixation is energetically demanding, the ability to carry out this process is widespread amongst prokaryotes.  
i5 However, it is controlled by several factors such as temperature, light, nutrients and trace metals such as iron and molybdenum  
i6 (Sohm et al., 2011; Tang et al., 2019). Oceanic N<sub>2</sub> fixation is the major source of nitrogen to the marine system (Karl et al.,  
i7 2002; Gruber and Sarmiento, 1997), thus, diazotrophs determine the biological productivity of our planet (Falkowski et al.  
i8 (2008), impact the global carbon cycle and the formation of organic matter (Galloway et al., 2004; Zehr and Capone, 2020).  
i9 Traditionally it has been believed that the distribution of diazotrophs was limited to warm and oligotrophic waters (Buchanan  
i0 et al., 2019; Sohm et al., 2011; Luo et al., 2012) until putative diazotrophs were identified in the central Arctic Ocean and  
i1 Baffin Bay (Farnelid et al., 2011; Damm et al., 2010). First rate measurements have been reported for the Canadian Arctic by  
i2 Blais et al. (2012) and recent studies have reported rate measurements in adjacent seas (Harding et al., 2018; Sipler et al., 2017;  
i3 Shiozaki et al., 2017, 2018), drawing attention to cold and temperate waters as significant contributors to the global nitrogen  
i4 budget through diverse organisms.

i5 UCYN-A has been described as the dominant active N<sub>2</sub> fixing cyanobacterial diazotroph in arctic waters (Harding et al.  
i6 (2018)), while other cyanobacteria have only occasionally been reported (Diez et al., 2012; Fernández-Méndez et al., 2016; Blais  
i7 et al.,) However, other recent studies suggest that the majority of the arctic marine diazotrophs are NCDs (non-cyanobacterial  
i8 diazotroph) and those may contribute significantly to N<sub>2</sub> fixation in the Arctic Ocean (Shiozaki et al., 2018; Fernández-Méndez  
i9 et al., 2016; Harding et al., 2018; Von Friesen and Rie- mann, 2020). Recent work by Robicheau et al. (2023) nearby Baffin Bay,  
i0 geographically close to the sampling area, document low *npH* gene abundance while still detecting diazotrophs in Arctic surface waters,  
i1 highlighting the patchy distribution of diazotrophs across Arctic coastal environments. Studies on the Arctic diazotroph community  
i2 remain scarce, leaving Arctic environments poorly understood regarding N<sub>2</sub> fixation. Shao et al. (2023) note the impossibility  
i3 of estimating Arctic N<sub>2</sub> fixation rates due to the sparse spatial coverage, which currently represents only approximately 1 % of  
i4 the Arctic Ocean. Increasing data coverage in future studies will aid in better constraining the contribution of N<sub>2</sub> fixation to  
i5 the global oceanic nitrogen budget (Tang et al. (2019)).

i6 The Arctic ecosystem is undergoing significant changes driven by rising temperatures and the accelerated melting of sea ice, a  
i7 trend predicted to intensify in the future (Arrigo et al., 2008; Hanna et al., 2008; Haine et al., 2015). These climate-driven shifts  
i8 have stimulated primary productivity in the Arctic by 57 % from 1998 to 2018, elevating nutrient demands in the Arctic Ocean  
i9 (Ardyna and Arrigo, 2020; Arrigo and van Dijken, 2015; Lewis et al., 2020). This increase is attributed to prolonged  
i0 phytoplankton growing seasons and expanding ice-free areas suitable for phytoplankton growth (Arrigo et al. (2008)).  
i1 However, despite these dramatic changes, the role of N<sub>2</sub> fixation in sustaining Arctic primary production remains poorly  
i2 understood. While recent studies suggest that diazotrophic activity may contribute to nitrogen inputs in polar regions (Sipler  
i3 et al. (2017)), fundamental uncertainties remain regarding the extend, distribution and environmental drivers of N<sub>2</sub> Fixation in  
i4 the Arctic Ocean. Specifically, it is unclear whether increased glacial meltwater input enhances or inhibits N<sub>2</sub> Fixation through  
i5 changes in nutrient availability, stratification, and microbial community composition. Thus, the question of whether nitrogen  
i6 limitation will emerge as a key factor constraining Arctic primary production under future climate scenarios remains unresolved. In this  
i7 study, we investigate the diversity of diazotrophic communities alongside in situ N<sub>2</sub> fixation rate measurements in Disko Bay

**Deleted:** N<sub>2</sub> fixation is performed by diverse group of cyanobacteria as well as by non-cyanobacteria diazotrophs (NCDs).

**Deleted:** in those waters

**Deleted:** while

**Deleted:** 2012).

**Deleted:** R

**Deleted:** found

**Formatted:** Font: Italic

**Deleted:** Still, s

**Deleted:** Additionally, t

**Deleted:** consequent reduc- tion

**Deleted:** in

**Formatted:** Indent: Left: 0,14 cm, Right: 0,66 cm

**Deleted:** extent due to accelerated melting, which is

**Deleted:** increase

**Deleted:** severe

**Deleted:** thereby

**Deleted:** can be

**Deleted:** the extension of the

**Deleted:** the

**Deleted:** sion of

**Deleted:**

**Deleted:** available

**Deleted:** The Greenland Ice Sheet is strongly affected by climate change and the waters of Baffin Bay have experienced a substantial sea surface temperature (SST) increase of 47.4 % along with a significant increase in chlorophyll a (Chl a) concentration of 26.4 % over the last two decades (1998–2018) (Lewis et al. (2020)). Coastal sites are particularly impacted by melting, receiving glacial runoff enriched with nutrients and trace elements triggering phytoplankton blooms and altering near-shore biogeochemical cycling (Ardyna and Arrigo, 2020; Arrigo et al., 2017; Hendry et al., 2019; Bhatia et al., 2013).

(Qeqertarsuaq), a coastal Arctic system strongly influenced by glacial meltwater input. By linking environmental parameters to N<sub>2</sub> fixation dynamics, we aim to clarify the role of diazotrophs in Arctic nutrient cycling and assess their potential contribution to sustaining primary production in a changing Arctic. Understanding these processes is essential for refining biogeochemical models and predicting ecosystem responses to future climate change.

## 2 Material and methods

### 2.1 Seawater sampling

The research expedition was conducted from August 16 to 26 in 2022 aboard the Danish military vessel P540 within the waters of Qeqertarsuaq, located in the western region of Greenland (Kalaallit Nunaat). Discrete water samples were obtained using a 10 L Niskin bottle, manually lowered with a hand winch to five distinct depths (surface, 5, 25, 50, and 100 m). A comprehensive sampling strategy was employed at 10 stations (Fig. 1), covering the surface to a depth of 100 m. The sampled parameters included water characteristics, such as nutrient concentrations, chl *a*, particulate organic carbon (POC) and nitrogen (PON), molecular samples for nucleic acid extractions (DNA), dissolved inorganic carbon (DIC) as well as CTD sensor data. At three selected stations (3,7,10) N<sub>2</sub> fixation and primary production rates were quantified through concurrent incubation experiments. Samples for nutrient analysis, nitrate (NO<sub>3</sub><sup>-</sup>), nitrite (NO<sub>2</sub><sup>-</sup>) and phosphate (PO<sub>4</sub><sup>3-</sup>) were taken in triplicates, filtered through a 0.22  $\mu$ m syringe filter (Avantor VWR® Radnor, Pa, USA) and stored at -20 °C until further analysis. Concentrations were spectrophotometrically determined (Thermo Scientific, Genesys 10S UV-VIS spectrophotometer) following the established protocols of Murphy and Riley (1962) for PO<sub>4</sub><sup>3-</sup>; García-Robledo et al. (2014) for NO<sub>3</sub><sup>-</sup> & NO<sub>2</sub><sup>-</sup> (detection limits: 0.01  $\mu$ mol L<sup>-1</sup> (NO<sub>3</sub><sup>-</sup>, NO<sub>2</sub><sup>-</sup>, and PO<sub>4</sub><sup>3-</sup>), 0.05  $\mu$ mol L<sup>-1</sup> (NH<sub>4</sub><sup>+</sup>)). Chl *a* samples were filtered onto 47 mm  $\phi$  GF/F filters (GE Healthcare Life Sciences, Whatman, USA), placed into darkened 15 mL LightSafe centrifuge tubes (Merck, Rahway, NJ, USA) and were subsequently stored at -20 °C until further analysis. To determine the Chl *a* concentration, the samples were immersed in 8 mL of 90 % acetone overnight at 5 °C. Subsequently, 1 mL of the resulting solution was transferred to a 1.5 mL glass vial (Mikrolab Aarhus A/S, Aarhus, Denmark) the following day and subjected to analysis using the Trilogy® Fluorometer (Model #7200-00) equipped with a Chl *a* in vivo blue module (Model #7200-043, both Turner Designs, San Jose, CA, USA). Measurements of serial dilutions from a 4 mg L<sup>-1</sup> stock standard and 90 % acetone (serving as blank) were performed to calibrate the instrument. In addition, measurements of a solid-state secondary standard were performed every 10 samples. Water (1 L) water from each depth was filtered for the determination of POC and PON concentrations, as well as natural isotope abundance ( $\delta$  <sup>13</sup>C POC /  $\delta$  <sup>15</sup>N PON) using 47 mm  $\phi$ , 0.7  $\mu$ m nominal pore size precombusted GF/F filter (GE Healthcare Life Sciences, Whatman, USA), which were subsequently stored at -20 °C until further analysis. Seawater samples for DNA were filtered through 47 mm  $\phi$ , 0.22  $\mu$ m MCE membrane filter (Merck, Millipore Ltd., Ireland) for a maximum of 20 minutes, employing a gentle vacuum (200 mbar). The filtered volumes varied depending on the amount of material captured on the filter, ranging from 1.3 L to 2 L, with precise measurements recorded. The filters were promptly stored at -20 °C on the ship and moved to -80 °C upon arrival to the lab until further analysis.

**Deleted:** Given the changes, there is an urgency to explore the role of N<sub>2</sub> fixation in shaping the response of the Arctic ecosystem to these environmental changes. While the general magnitude of N<sub>2</sub> fixation is suspected to have a substantial impact (Sipler et al. (2017)), the complexity of Arctic biogeochemical processes necessitates further studies and broader spatial and temporal investigations to facilitate robust predictions. The question of whether primary

**Deleted:** production in the Arctic will be limited by nitrogen availability and the extent to which species will adapt to these conditions remains unknown and needs to be addressed. This study aims to contribute to the understanding of N<sub>2</sub> fixation dynamics and its implications for ecosystem productivity with the rapidly evolving Arctic Ocean.

We explored the diazotroph diversity in combination with N<sub>2</sub> fixation rate measurements, to elucidate the importance of this process in the Arctic ecosystem. We hope that understanding the dynamics of N<sub>2</sub> fixation and its impact on the ecosystem productivity can inform predictions and help managing the consequences of ongoing environmental changes in the Arctic Ocean. Our study has been carried out in Disko Bay (Qeqertarsuaq), which can serve as a model for Arctic coastal systems influenced by large meltwater runoff and thus potentially an addition of high levels of iron and nutrients, both of which have the ability to affect N<sub>2</sub> fixation (Lewis et al., 2020; Bhatia et al., 2013).

**Deleted:** -

**Formatted:** Superscript

**Formatted:** Subscript

**Formatted:** Superscript

**Formatted:** Subscript

**Formatted:** Superscript

**Formatted:** Subscript

**Formatted:** Superscript

**Formatted:** Superscript

**Formatted:** Subscript

**Formatted:** Superscript

**Deleted:** -

**Deleted:**

**Deleted:** Seawater (40 ml) was filtered through a 0.22  $\mu$ m syringe filter (Avantor VWR® Radnor, Pa, USA) and stored at 4 °C in an amber glass vial, sealed with closed caps, affixed with a PTFE-faced silicon liner (Thermo Fisher Scientific, Waltham, MA, USA) for subsequent DIC measurements in the laboratory using an AS-C5 DIC analyzer (ApolloSciTech, Newark, Delaware, USA) equipped with a laser-based CO<sub>2</sub> detector. Sample anal... [11]

16 To achieve detailed vertical profiles, a conductivity-temperature-depth-profiler (CTD, Seabird X) equipped with supplemen-  
17 tary sensors for dissolved oxygen (DO), photosynthetic active radiation (PAR), and fluorescence (Fluorometer) was manually  
18 deployed.

## 19 2.2 Nitrogen fixation and primary production

0 Water samples were collected at three distinct depths (0, 25 and 50 m) for the investigation of N<sub>2</sub> fixation rates and primary  
1 production rates, encompassing the euphotic zone, chlorophyll maximum, and a light-absent zone. Three incubation stations  
2 (Fig. 2: station 3, 7, 10) were chosen, in a way to cover the variability of the study area. This strategic sampling aimed to  
3 capture a gradient of the water column with varying environmental conditions, relevant to the aim of the study. N<sub>2</sub> fixation  
4 rates were assessed through triplicate incubations employing the modified <sup>15</sup>N-N<sub>2</sub> dissolution technique after Großkopf et al.  
5 (2012) and Mohr et al. (2010).

6 To ensure minimal contamination, 2.3 L glass bottles (Schott-Duran, Wertheim, Germany) underwent pre-cleaning and acid  
7 washing before being filled with seawater samples. Oxygen contamination during sample collection was mitigated by gently  
8 and bubble-free filling the bottles from the bottom, allowing the water to overflow. Each incubation bottle received a 100 mL  
9 amendment of <sup>15</sup>N-N<sub>2</sub> enriched seawater (98 %, Cambridge Isotope Laboratories, Inc., USA) achieving an average dissolved  
10 N<sub>2</sub> isotope abundance (<sup>15</sup>N atom %) of  $3.90 \pm 0.02$  atom % (mean  $\pm$  SD). Additionally, 1 mL of H<sup>13</sup>CO<sub>3</sub> (1 g/50 mL) (Sigma-  
11 Aldrich, Saint Louis Missouri US) was added to each incubation bottle, roughly corresponding to 10 atom % enrichment and  
12 thus measurements of primary production and N<sub>2</sub> fixation were conducted in the same bottle. Following the addition of both  
13 isotopic components, the bottles were closed airtight with septa-fitted caps and incubated for 24 hours on-deck incubators with  
14 a continuous surface seawater flow. These incubators, partially shaded ([using daylight-filtering foil](#)) to simulate in situ  
15 photosynthetically active radiation (PAR) conditions, aimed to replicate environmental parameters experienced at the sampled  
16 depths. Control incubations utilizing atmospheric air served as controls to monitor any natural changes in  $\delta$  <sup>15</sup>N not attributable  
17 to <sup>15</sup>N-N<sub>2</sub> addition. These control incubations were conducted using the dissolution method, like the <sup>15</sup>N-N<sub>2</sub> enrichment  
18 experiments, but with the substitution of atmospheric air instead of isotopic tracer.

19 After the incubation period, subsamples for nutrient analysis were taken from each incubation sample, and the remaining  
0 content was subjected to the filtration process and were gently filtered (200 mbar) onto precombusted GF/F filters (Advantec,  
1 47 mm  $\varnothing$ , 0.7  $\mu$ m nominal pore size). This step ensured a comprehensive examination of both nutrient dynamics and the  
2 isotopic composition of the particulate pool in the incubated samples. Samples were stored at -20 °C until further analysis.

3 Upon arrival in the lab, the filters were dried at 60 °C and to eliminate particulate inorganic carbon, subsequently subject to acid  
4 fuming during which they were exposed to concentrated hydrochloric acid (HCL) vapors overnight in a desiccator. After  
5 undergoing acid treatment, the filters were carefully dried, then placed into tin capsules and pelletized for subsequent analysis.  
6 The determination of POC and PON, as well as isotopic composition ( $\delta$  <sup>13</sup>C POC /  $\delta$  <sup>15</sup>N PON), was carried out using an  
7 elemental analyzer (Flash EA, ThermoFisher, USA) connected to a mass spectrometer (Delta V Advantage Isotope Ratio MS,  
8 ThermoFisher, USA) with the ConFlo IV interface. This analytical setup was applied to all filters. These values, derived from

**Deleted:** In the same manner, discrete water samples were obtained using a 10 L Niskin bottle, manually lowered with a hand winch to five distinct depths (Surface, 5, 25, 50, 100 m). These systematic and multifaceted sampling methodologies provide a robust dataset for a comprehensive analysis of the hydrographic conditions in Qeqertarsuaq.

**Formatted:** Indent: Left: 0,15 cm, Right: 0,36 cm, Space Before: 0,7 pt

|6 triplicate incubation measurements, exhibited no omission of data points or identification of outliers. Final rate calculations for N<sub>2</sub>  
|7 fixation rates were performed after Mohr et al. (2010) and primary production rates after Slawyk et al. (1977). [A detailed](#)  
|8 [sensitivity analysis for N<sub>2</sub> fixation rates and the contribution of each source of error of all parameters can be found as a](#)  
|9 [supplementary table.](#)

|0 **2.3 Molecular methods**

|1 The filters were flash-frozen in liquid nitrogen, crushed and DNA was extracted using the Qiagen DNA/RNA AllPrep Kit (Qi-  
|2 agen, Hildesheim, DE), following the procedure outlined by the manufacturer. The concentration and quality of the extracted  
|3 DNA was assessed spectrophotometrically using a MySpec spectrofluorometer (VWR, Darmstadt, Germany). The prepara-  
|4 tion of the metagenome library and sequencing were performed by BGI (China). Sequencing libraries were generated using  
|5 MGIEasy Fast FS DNA Library Prep Set following the manufacturer's protocol. Sequencing was conducted with 2x150bp on  
|6 a DNBSEQ-G400 platform (MGI). SOAPnuke1.5.5 (Chen et al. (2018)) was used to filter and trim low quality reads and  
|7 adaptor contaminants from the raw sequence reads, as clean reads. In total, fifteen metagenomic datasets were produced with  
|8 an average of 9.6G bp per sample.

|9 **2.3.1 Metagenomic De Novo assembly, gene prediction, and annotation**

|0 Megahit v1.2.9 (Li et al. (2015)) was used to assemble clean reads for each dataset with its minimum contig length as 500.  
|1 Prodigal v2.6.3 (Hyatt et al. (2010)) with the setting of “-p meta” was then used to predict the open reading frames (ORFs) of  
|2 the assembled contigs. ORFs from all the available datasets were filtered (>100bp), dereplicated and merged into a catalog of  
|3 non-redundant genes using cd-hit-est (>95 % sequence identity) (Fu et al. (2012)). Salmon v1.10.0 (Patro et al. (2017)) with  
|4 the “- meta” option was employed to map clean reads of each dataset to the catalog of non-redundant genes and generate the  
|5 GPM (genes per million reads) abundance. Eggnog mapper v2.1.12 (Cantalapiedra et al. (2021)) was then performed to assign  
|6 KEGG Orthology (KO) and identify specific functional annotation for the catalog of non-redundant genes. The marker genes,  
|7 *nifDK* (K02586, K02591 nitrogenase molybdenum-iron protein alpha/beta chain) and *nifH* (K02588, nitrogenase iron protein),  
|8 were used for the evaluation of microbial potential of N<sub>2</sub> fixation. *RbcL* (K01601, ribulose-bisphosphate carboxylase large  
|9 chain) and *psba* (K02703, photosystem II P680 reaction center D1 protein) were selected to evaluate the microbial potential  
|0 of carbon fixation and photosynthesis, respectively. [The molecular datasets have been deposited with the accession number:](#)  
|1 [Bioproject PRJNA1133027.](#)

|2 **3 Results and discussion**

|3 **3.1 Hydrographic conditions in Qeqertarsuaq (Disco Bay) and Sullorsuaq (Vaigat) Strait**

|4 Disko Bay (Qeqertarsuaq) is located along the west coast of Greenland (Kalaallit Nunaat) at approximately 69 °N (Figure 1),  
|5 and is strongly influenced by the West Greenland Current (WGC) which is associated with the broader Baffin Bay Polar Waters  
|6 (BBPW) (Mortensen et al., 2022; Hansen et al., 2012). The WGC does not only significantly shape the hydrographic conditions

Formatted: Indent: Left: 0,14 cm, Right: 0,66 cm, Space Before: 0,05 pt

Field Code Changed

Field Code Changed

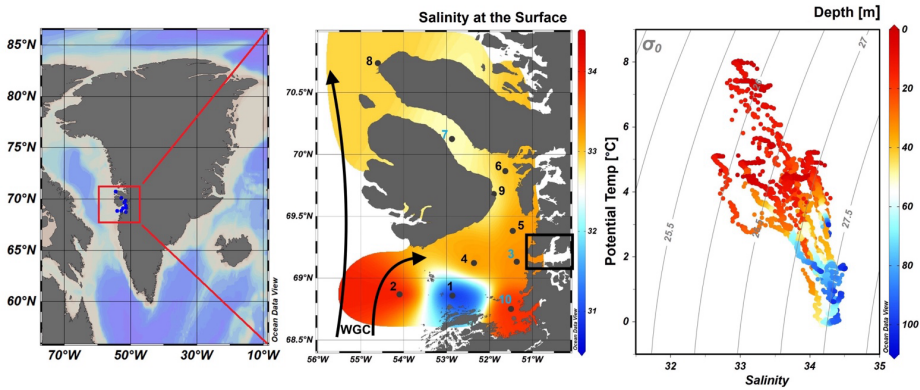
Deleted: ,

Deleted: ¶

Formatted: Font: 10 pt

3 within the bay but also plays an important role in the larger context of Greenland Ice Sheet melting (Mortensen et al. (2022)).  
 4 Central to the hydrographic system of the Qeqertarsuaq area is the Jakobshavn Isbræ, which is the most productive glacier in  
 5 the northern hemisphere and believed to drain about 7 % of the Greenland Ice Sheet and thus contributes substantially to the  
 6 water influx into the Qeqertarsuaq (Holland et al. (2008)). A predicted increased inflow of warm subsurface water, originating  
 7 from North Atlantic waters, has been suggested to further affect the melting of the Jakobshavn Isbræ and thus adds another  
 8 layer of complexity to this dynamic system (Holland et al., 2008; Hansen et al., 2012).

9 The hydrographic conditions in Qeqertarsuaq have a significant influence on biological processes, nutrient availability, and the

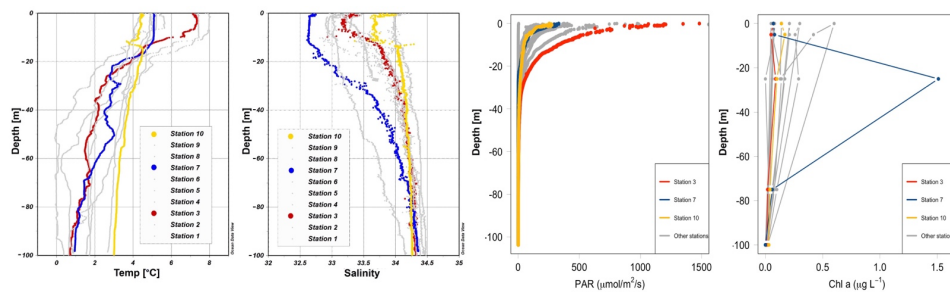


1 **Figure 1.** Map of Greenland (Kalaallit Nunaat) with indication of study area (red box), on the left. Interpolated distribution of Sea Surface  
 2 Salinity (SSS) values with corresponding isosurface lines and indication of 10 sampled stations (normal stations in black, incubation stations  
 3 in blue), **black arrows indicate the West Greenland Current (WGC)** and the black box indicate the location of the Jakobshavn Isbræ, in the  
 4 middle. Scatterplot of the potential temperature and salinity for all station data. The plot is used for the identification of the main water  
 5 masses within the study area. Isopleths ( $\text{kg m}^{-3}$ ) are depicted in grey lines, on the right. Figures were created in Ocean Data View (ODV)  
 6 (Schlitzer (2022)).

7 broader marine ecosystem (Munk et al., 2015; Hendry et al., 2019; Schiott, 2023).

8 During our survey, we found very heterogenous hydrographic conditions at the different stations across Qeqertarsuaq (Fig. 1 &  
 9 Fig. 2). The three selected stations for  $\text{N}_2$  fixation analysis (stations 3, 7, and 10) were strategically chosen to capture the spatial  
 10 variability of the area. Surface salinity and temperature measurements at these stations indicate the influence of freshwater  
 11 input. The surface temperature exhibit a range of 4.5 to 8 °C, while surface salinity varies between 31 and 34, as illustrated in  
 12 Fig. 1. The profiles sampled during our survey extend to a maximum depth of 100 m. Comparison of temperature/salinity (T/S)  
 13 plots with recent studies suggests the presence of previously described water masses, including Warm Fjord Water (WFjW)  
 14

17 and Cold Fjord Water (CFjW) with an overlaying surface glacial meltwater runoff. Those water masses are defined with a  
18 density range of  $27.20 \leq \sigma_0 \leq 27.31$  but different temperature profiles. Thus water masses can be differentiated by their  
19 temperature within the same density range (Gladish et al. (2015)). Other water masses like upper subpolar mode water  
0 (uSPMW), deep subpolar mode water (dSPMW) and Baffin Bay polar Water (BBPW) which has been identified in the Disko  
1 Bay (Qeqertarsuaq) before, cannot be identified from this data and may be present in deeper layers (Mortensen et al., 2022;  
2 Sherwood et al., 2021; Myers and Ribergaard, 2013; Rysgaard et al., 2020). The temperature and salinity profiles across the 10



3  
4  
5  
6 **Figure 2.** Profiles of temperature (°C), salinity, photosynthetically active radiation (PAR) (μmol/m<sup>2</sup>/s) and Chl *a* (mg m<sup>-3</sup>) across stations 1 to  
7 10 with depth (m). Stations 3, 7, and 10 are highlighted in red, blue, and yellow, respectively, to emphasize incubation stations. Figures were  
8 created in Ocean Data View and R-Studio (Schlitzer (2022)).

9 stations in the study area show distinct stratification and variability, which is represented through the three incubation stations  
10 (highlighted stations 3, 7, and 10 in Fig. 2). They display varying degrees of stratification and mixing, with notable differences  
11 in the salinity and temperature profiles. Station 3 and station 7 exhibit clear stratification in both temperature and salinity  
12 marked by the presence of thermoclines and haloclines. These features suggest significant freshwater input influenced by local  
13 weather conditions and climate dynamics, like surface heat absorption. In contrast, Station 10 exhibits a narrower range of  
14 temperature and salinity values throughout the water column compared to Stations 3 and 7, indicating more well-mixed  
15 conditions. This uniformity is likely influenced by the regional circulation pattern and partial upwelling (Hansen et al., 2012;  
16 Krawczyk et al., 2022). The distinct characteristics observed at station 10, as illustrated in the surface plot (Fig. 1), show an  
17 elevated salinity and colder temperatures compared

18 to the other stations. This feature suggests upwelling of deeper waters along the shallower shelf, likely facilitated by the local  
19 seafloor topography. Specifically, the seafloor shallowing off the coast of Station 10 may act as a barrier, disrupting typical  
0 circulation and forcing deeper, saltier, and colder waters to the surface. This pattern aligns with previous studies that describe  
1 similar mechanisms in the region (Krawczyk et al. (2022)). Their description of the bathymetry in Qeqertarsuaq, featuring  
2 depths ranging from ca. 50 to 900 m, suggests its impact on turbulent circulation patterns, leading to the mixing of different

3  
4  
5  
6  
7  
8  
9  
10  
11  
12  
13  
14  
15  
16  
17  
18  
19  
20  
21  
22  
23  
24  
25  
26  
27  
28  
29  
30  
31  
32  
33  
34  
35  
36  
37  
38  
39  
40  
41  
42  
43  
44  
45  
46  
47  
48  
49  
50  
51  
52  
53  
54  
55  
56  
57  
58  
59  
60  
61  
62  
63  
64  
65  
66  
67  
68  
69  
70  
71  
72  
73  
74  
75  
76  
77  
78  
79  
80  
81  
82  
83  
84  
85  
86  
87  
88  
89  
90  
91  
92  
93  
94  
95  
96  
97  
98  
99  
100  
101  
102  
103  
104  
105  
106  
107  
108  
109  
110  
111  
112  
113  
114  
115  
116  
117  
118  
119  
120  
121  
122  
123  
124  
125  
126  
127  
128  
129  
130  
131  
132  
133  
134  
135  
136  
137  
138  
139  
140  
141  
142  
143  
144  
145  
146  
147  
148  
149  
150  
151  
152  
153  
154  
155  
156  
157  
158  
159  
160  
161  
162  
163  
164  
165  
166  
167  
168  
169  
170  
171  
172  
173  
174  
175  
176  
177  
178  
179  
180  
181  
182  
183  
184  
185  
186  
187  
188  
189  
190  
191  
192  
193  
194  
195  
196  
197  
198  
199  
200  
201  
202  
203  
204  
205  
206  
207  
208  
209  
210  
211  
212  
213  
214  
215  
216  
217  
218  
219  
220  
221  
222  
223  
224  
225  
226  
227  
228  
229  
230  
231  
232  
233  
234  
235  
236  
237  
238  
239  
240  
241  
242  
243  
244  
245  
246  
247  
248  
249  
250  
251  
252  
253  
254  
255  
256  
257  
258  
259  
260  
261  
262  
263  
264  
265  
266  
267  
268  
269  
270  
271  
272  
273  
274  
275  
276  
277  
278  
279  
280  
281  
282  
283  
284  
285  
286  
287  
288  
289  
290  
291  
292  
293  
294  
295  
296  
297  
298  
299  
300  
301  
302  
303  
304  
305  
306  
307  
308  
309  
310  
311  
312  
313  
314  
315  
316  
317  
318  
319  
320  
321  
322  
323  
324  
325  
326  
327  
328  
329  
330  
331  
332  
333  
334  
335  
336  
337  
338  
339  
340  
341  
342  
343  
344  
345  
346  
347  
348  
349  
350  
351  
352  
353  
354  
355  
356  
357  
358  
359  
360  
361  
362  
363  
364  
365  
366  
367  
368  
369  
370  
371  
372  
373  
374  
375  
376  
377  
378  
379  
380  
381  
382  
383  
384  
385  
386  
387  
388  
389  
390  
391  
392  
393  
394  
395  
396  
397  
398  
399  
400  
401  
402  
403  
404  
405  
406  
407  
408  
409  
410  
411  
412  
413  
414  
415  
416  
417  
418  
419  
420  
421  
422  
423  
424  
425  
426  
427  
428  
429  
430  
431  
432  
433  
434  
435  
436  
437  
438  
439  
440  
441  
442  
443  
444  
445  
446  
447  
448  
449  
450  
451  
452  
453  
454  
455  
456  
457  
458  
459  
460  
461  
462  
463  
464  
465  
466  
467  
468  
469  
470  
471  
472  
473  
474  
475  
476  
477  
478  
479  
480  
481  
482  
483  
484  
485  
486  
487  
488  
489  
490  
491  
492  
493  
494  
495  
496  
497  
498  
499  
500  
501  
502  
503  
504  
505  
506  
507  
508  
509  
510  
511  
512  
513  
514  
515  
516  
517  
518  
519  
520  
521  
522  
523  
524  
525  
526  
527  
528  
529  
530  
531  
532  
533  
534  
535  
536  
537  
538  
539  
540  
541  
542  
543  
544  
545  
546  
547  
548  
549  
550  
551  
552  
553  
554  
555  
556  
557  
558  
559  
5510  
5511  
5512  
5513  
5514  
5515  
5516  
5517  
5518  
5519  
5520  
5521  
5522  
5523  
5524  
5525  
5526  
5527  
5528  
5529  
5530  
5531  
5532  
5533  
5534  
5535  
5536  
5537  
5538  
5539  
55310  
55311  
55312  
55313  
55314  
55315  
55316  
55317  
55318  
55319  
55320  
55321  
55322  
55323  
55324  
55325  
55326  
55327  
55328  
55329  
55330  
55331  
55332  
55333  
55334  
55335  
55336  
55337  
55338  
55339  
55340  
55341  
55342  
55343  
55344  
55345  
55346  
55347  
55348  
55349  
55350  
55351  
55352  
55353  
55354  
55355  
55356  
55357  
55358  
55359  
55360  
55361  
55362  
55363  
55364  
55365  
55366  
55367  
55368  
55369  
55370  
55371  
55372  
55373  
55374  
55375  
55376  
55377  
55378  
55379  
55380  
55381  
55382  
55383  
55384  
55385  
55386  
55387  
55388  
55389  
55390  
55391  
55392  
55393  
55394  
55395  
55396  
55397  
55398  
55399  
553100  
553101  
553102  
553103  
553104  
553105  
553106  
553107  
553108  
553109  
553110  
553111  
553112  
553113  
553114  
553115  
553116  
553117  
553118  
553119  
553120  
553121  
553122  
553123  
553124  
553125  
553126  
553127  
553128  
553129  
553130  
553131  
553132  
553133  
553134  
553135  
553136  
553137  
553138  
553139  
553140  
553141  
553142  
553143  
553144  
553145  
553146  
553147  
553148  
553149  
553150  
553151  
553152  
553153  
553154  
553155  
553156  
553157  
553158  
553159  
553160  
553161  
553162  
553163  
553164  
553165  
553166  
553167  
553168  
553169  
553170  
553171  
553172  
553173  
553174  
553175  
553176  
553177  
553178  
553179  
553180  
553181  
553182  
553183  
553184  
553185  
553186  
553187  
553188  
553189  
553190  
553191  
553192  
553193  
553194  
553195  
553196  
553197  
553198  
553199  
553200  
553201  
553202  
553203  
553204  
553205  
553206  
553207  
553208  
553209  
553210  
553211  
553212  
553213  
553214  
553215  
553216  
553217  
553218  
553219  
553220  
553221  
553222  
553223  
553224  
553225  
553226  
553227  
553228  
553229  
553230  
553231  
553232  
553233  
553234  
553235  
553236  
553237  
553238  
553239  
553240  
553241  
553242  
553243  
553244  
553245  
553246  
553247  
553248  
553249  
553250  
553251  
553252  
553253  
553254  
553255  
553256  
553257  
553258  
553259  
553260  
553261  
553262  
553263  
553264  
553265  
553266  
553267  
553268  
553269  
553270  
553271  
553272  
553273  
553274  
553275  
553276  
553277  
553278  
553279  
553280  
553281  
553282  
553283  
553284  
553285  
553286  
553287  
553288  
553289  
553290  
553291  
553292  
553293  
553294  
553295  
553296  
553297  
553298  
553299  
553300  
553301  
553302  
553303  
553304  
553305  
553306  
553307  
553308  
553309  
553310  
553311  
553312  
553313  
553314  
553315  
553316  
553317  
553318  
553319  
553320  
553321  
553322  
553323  
553324  
553325  
553326  
553327  
553328  
553329  
553330  
553331  
553332  
553333  
553334  
553335  
553336  
553337  
553338  
553339  
553340  
553341  
553342  
553343  
553344  
553345  
553346  
553347  
553348  
553349  
553350  
553351  
553352  
553353  
553354  
553355  
553356  
553357  
553358  
553359  
553360  
553361  
553362  
553363  
553364  
553365  
553366  
553367  
553368  
553369  
553370  
553371  
553372  
553373  
553374  
553375  
553376  
553377  
553378  
553379  
553380  
553381  
553382  
553383  
553384  
553385  
553386  
553387  
553388  
553389  
553390  
553391  
553392  
553393  
553394  
553395  
553396  
553397  
553398  
553399  
553400  
553401  
553402  
553403  
553404  
553405  
553406  
553407  
553408  
553409  
553410  
553411  
553412  
553413  
553414  
553415  
553416  
553417  
553418  
553419  
553420  
553421  
553422  
553423  
553424  
553425  
553426  
553427  
553428  
553429  
553430  
553431  
553432  
553433  
553434  
553435  
553436  
553437  
553438  
553439  
553440  
553441  
553442  
553443  
553444  
553445  
553446  
553447  
553448  
553449  
553450  
553451  
553452  
553453  
553454  
553455  
553456  
553457  
553458  
553459  
553460  
553461  
553462  
553463  
553464  
553465  
553466  
553467  
553468  
553469  
553470  
553471  
553472  
553473  
553474  
553475  
553476  
553477  
553478  
553479  
553480  
553481  
553482  
553483  
553484  
553485  
553486  
553487  
553488  
553489  
553490  
553491  
553492  
553493  
553494  
553495  
553496  
553497  
553498  
553499  
553500  
553501  
553502  
553503  
553504  
553505  
553506  
553507  
553508  
553509  
553510  
553511  
553512  
553513  
553514  
553515  
553516  
553517  
553518  
553519  
553520  
553521  
553522  
553523  
553524  
553525  
553526  
553527  
553528  
553529  
553530  
553531  
553532  
553533  
553534  
553535  
553536  
553537  
553538  
553539  
553540  
553541  
553542  
553543  
553544  
553545  
553546  
553547  
553548  
553549  
553550  
553551  
553552  
553553  
553554  
553555  
553556  
553557  
553558  
553559  
553560  
553561  
553562  
553563  
553564  
553565  
553566  
553567  
553568  
553569  
553570  
553571  
553572  
553573  
553574  
553575  
553576  
553577  
553578  
553579  
553580  
553581  
553582  
553583  
553584  
553585  
553586  
553587  
553588  
553589  
553590  
553591  
553592  
553593  
553594  
553595  
553596  
553597  
553598  
553599  
553600  
553601  
553602  
553603  
553604  
553605  
553606  
553607  
553608  
553609  
553610  
553611  
553612  
553613  
553614  
553615  
553616  
553617  
553618  
553619  
553620  
553621  
553622  
553623  
553624  
553625  
553626  
553627  
553628  
553629  
553630  
553631  
553632  
553633  
553634  
553635  
553636  
553637  
553638  
553639  
553640  
553641  
553642  
553643  
553644  
553645  
553646  
553647  
553648  
553649  
553650  
553651  
553652  
553653  
553654  
553655  
553656  
553657  
553658  
553659  
553660  
553661  
553662  
553663  
553664  
553665  
553666  
553667  
553668  
553669  
553670  
553671  
553672  
553673  
553674  
553675  
553676  
553677  
553678  
553679  
553680  
553681  
553682  
553683  
553684  
553685  
553686  
553687  
553688  
553689  
553690  
553691  
553692  
553693  
553694  
553695  
553696  
553697  
553698  
553699  
553700  
553701  
553702  
553703  
553704  
553705  
553706  
553707  
553708  
553709  
553710  
553711  
553712  
553713  
553714  
553715  
553716  
553717  
553718  
553719  
553720  
553721  
553722  
553723  
553724  
553725  
553726  
553727  
553728  
553729  
553730  
553731  
553732  
553733  
553734  
553735  
553736  
553737  
553738  
553739  
5537340  
5537341  
5537342  
5537343  
5537344  
5537345  
5537346  
5537347  
5537348  
5537349  
5537350  
5537351  
5537352  
5537353  
5537354  
5537355  
5537356  
5537357  
5537358  
5537359  
5537360  
5537361  
5537362  
5537363  
5537364  
5537365  
5537366  
5537367  
5537368  
5537369  
5537370  
5537371  
5537372  
5537373  
5537374  
5537375  
5537376  
5537377  
5537378  
5537379  
5537380  
5537381  
5537382  
5537383  
5537384  
5537385  
5537386  
5537387  
5537388  
5537389  
5537390  
5537391  
5537392  
5537393  
5537394  
5537395  
5537396  
5537397  
5537398  
5537399  
5537400  
5537401  
5537402  
5537403  
5537404  
5537405  
5537406  
5537407  
5537408  
5537409  
55374010  
55374011  
55374012  
55374013  
55374014  
55374015  
55374016  
55374017  
55374018  
55374019  
55374020  
55374021  
55374022  
55374023  
55374024  
55374025  
55374026  
55374027  
55374028  
55374029  
55374030  
55374031  
55374032  
55374033  
55374034  
55374035  
55374036  
55374037  
55374038  
55374039  
55374040  
55374041  
55374042  
55374043  
55374044  
55374045  
55374046  
55374047  
55374048  
55374049  
55374050  
55374051  
55374052  
55374053  
55374054  
55374055  
55374056  
55374057  
55374058  
55374059  
55374060  
55374061  
55374062  
55374063  
55374064  
55374065  
55374066  
55374067  
55374068  
55374069  
55374070  
55374071  
55374072  
55374073  
55374074  
55374075  
55374076  
55374077  
55374078  
55374079  
55374080  
55374081  
55374082  
55374083  
55374084  
55374085  
55374086  
55374087  
55374088  
55374089  
55374090  
55374091  
55374092  
55374093  
55374094  
55374095  
55374096  
55374097  
55374098  
55374099  
55374100  
55374101  
55374102  
55374103  
55374104  
55374105  
55374106  
55374107  
55374108  
55374109  
55374110  
55374111  
55374112  
55374113  
55374114  
55374115  
55374116  
55374117  
55374118  
55374119  
553741100  
553741101  
553741102  
553741103  
553741104  
553741105  
553741106  
553741107  
553741108  
553741109  
553741110  
553741111  
553741112  
553741113  
553741114  
553741115  
553741116  
553741117  
553741118  
553741119  
5537411100  
5537411101  
5537411102  
5537411103  
5537411104  
5537411105  
5537411106  
5537411107  
5537411108  
5537411109  
5537411110  
5537411111  
5537411112  
5537411113  
5537411114  
5537411115  
5537411116  
5537411117  
5537411118  
5537411119  
55374111100  
55374111101  
55374111102  
55374111103  
55374111104  
55374111105  
55374111106  
55374111107  
5

17 water masses. Evident variability in oceanographic conditions that can be observed throughout the study area occurs particularly  
18 along characteristic topographical features like steep slopes, canyons, and shallower areas. The summer melting of sea ice and  
19 glaciers introduces freshwater influxes that create distinct vertical and horizontal gradients in salinity and temperature in the  
20 Qeqertarsuaq area Hansen et al. (2012). Additionally, the accelerated melting of the Jakobshavn Isbraæ, influenced by the  
21 warmer inflow from the West Greenland Intermediate Current (WGIC), further alters the hydrographic conditions. Recent  
22 observations indicate significant warming and shoaling of the WGIC, potentially enabling it to overcome the sill separating the  
23 Ilulissat Fjord from the Qeqertarsuaq area (Hansen et al., 2012; Holland et al., 2008; Myers and Ribergaard, 2013). This shift  
24 intensifies glacier melting, driving substantial changes in the local ecological dynamics (Ardyna et al., 2014; Arrigo et al., 2008;  
25 Bhatia et al., 2013).

### 3.2 N<sub>2</sub> Fixation Rate Variability and Associated Environmental Conditions

1 We quantified N<sub>2</sub> fixation rates within the waters of Qeqertarsuaq, spanning from the surface to a depth of 50 m (Table 1). The  
2 rates ranged from 0.16 to 2.71 nmol N L<sup>-1</sup> d<sup>-1</sup> with all rates surpassing the minimum quantifiably rate (Appendix Table 1).  
3 Our findings represent rates at the upper range of those observed in the Arctic Ocean. Previous measurements in the region  
4 have been limited, with only one study in Baffin Bay by Blais et al. (2012), reporting rates of 0.02 nmol N L<sup>-1</sup> d<sup>-1</sup>, which are 1-  
5 2 orders of magnitude lower than our observations. Moreover, Sipler et al. (2017), reported rates in the coastal Chukchi Sea,  
6 with average values of 7.7 nmol N L<sup>-1</sup> d<sup>-1</sup>. These values currently represent some of the highest rates measured in Arctic shelf  
7 environments. Compared to these, our highest measured rate (2.71 nmol N L<sup>-1</sup> d<sup>-1</sup>) is lower, but still important, particularly  
8 considering the more Atlantic-influenced location of our study site. Sipler et al. (2017) also noted that a significant fraction of  
9 diazotrophs were <3 µm in size, suggesting that small unicellular diazotrophs play a dominant role in Arctic nitrogen fixation.  
10 Altogether, our data contribute to the growing evidence that N<sub>2</sub> fixation is a widespread and potentially significant nitrogen  
11 source across various Arctic regions. Simultaneous primary production rate measurements ranged from 0.07 to 3.79 µmol N L<sup>-1</sup>  
12 d<sup>-1</sup>, with the highest rates observed at station 7 and generally higher values in the surface layers. Employing Redfield  
13 stoichiometry, the measured N<sub>2</sub> fixation rates accounted for 0.47 to 2.6 % (averaging 1.57 %) of primary production at our  
14 stations. The modest contribution to primary production suggests that N<sub>2</sub> fixation does not exert a substantial influence on the  
15 productivity of these waters during the time of the sampling. Rather, our N<sub>2</sub> fixation rates suggest primary production to depend  
16 mostly on additional nitrogen sources including regenerated, meltwater or land based sources.

17 The N:P ratio, calculated as DIN to DIP, indicates a deficit in N for primary production based on Redfield stoichiometry (Fig.  
18 3). This aligns with findings presented by Jensen et al. (1999) and Tremblay and Gagnon (2009), who observed a similar nitro-  
19 gen limitation in this region. Such biogeochemical conditions would be expected to generate a niche for N<sub>2</sub> fixing organisms  
20 (Sohm et al. (2011)). While N<sub>2</sub> fixation did not chiefly sustain primary production during our sampling campaign, we hypoth-  
21 esize that N<sub>2</sub> fixation has the potential to play a role in bloom dynamics under certain conditions. As nitrogen availability  
22 decreases,

23 during a bloom, it may provide a niche for N<sub>2</sub> fixation, potentially helping to extend the productive period of the bloom period

Deleted: Elevated N<sub>2</sub> fixation rates might play a role in nutrient dynamics and bloom development

Formatted: Space Before: 0,05 pt, Line spacing: Multiple 1,44 li

Deleted: detection

Deleted: limit

Deleted: Compared to other European Arctic waters, our rates at the surface and at 25 m water depth fall within the reported range for Arctic estuarine stations (1.04 to 1.87 nmol N L<sup>-1</sup> d<sup>-1</sup>, (SD ± 0.76 to 1.19) and marine stations (0.11 to 0.12 nmol N L<sup>-1</sup> d<sup>-1</sup>, (SD ± 0.09 to 0.09) (Blais et al. (2012)). However, we observed some of the highest rates reported so far,<sup>1</sup> particularly at the surface.

Deleted: relatively

Deleted: may

Formatted: Right: 0,66 cm, Space Before: 0,1 pt

Deleted: the relatively high

Deleted: rates observed

Deleted: may

Deleted: 1

Deleted: ing

1 (Reeder et al. (2021)). Satellite data indicates that a fall bloom began in early August, following the annual spring bloom, as  
 2 described by Ardyna et al. (2014). This double bloom situation may be driven by increased melting and the subsequent input of  
 3 bioavailable nutrients and iron (Fe) from meltwater runoff (Arrigo et al., 2017; Hopwood et al., 2016; Bhatia et al., 2013). The  
 4 meltwater from the Greenland Ice Sheet is a significant source of Fe (Bhatia et al., 2013; Hawkings et al., 2015, 2014), which is  
 5 a limiting factor especially for diazotrophs (Sohm et al. (2011)). Consequently, it is plausible that Fe and nutrients from the  
 6 Isbræ glacier create favorable conditions for both bloom development and diazotroph activity in Qeqertarsuaq. However, we  
 7 emphasize that confirming a causal link between N<sub>2</sub> fixation and secondary bloom development requires further evidence, such  
 8 as time-series data on nutrient concentrations, diazotroph abundance, and bloom dynamics.

0 **Table 1.** N<sub>2</sub> fixation (nmol N L<sup>-1</sup> d<sup>-1</sup>), standard deviation (SD), primary productivity (PP;  $\mu\text{mol C L}^{-1} \text{d}^{-1}$ ), SD, percentage of estimated new  
 1 primary productivity (% New PP) sustained by N<sub>2</sub> fixation, dissolved inorganic nitrogen compounds (NO<sub>x</sub>), phosphorus (PO<sub>4</sub>), and the molar  
 2 nitrogen-to-phosphorus ratio (N:P) at stations 3, 7, and 10.

Station (no.)	Depth (m)	N <sub>2</sub> fixation (nmol N L <sup>-1</sup> d <sup>-1</sup> )	SD ( $\pm$ )	Primary Productivity ( $\mu\text{mol C L}^{-1} \text{d}^{-1}$ )	SD ( $\pm$ )	% New PP (%)	NO <sub>x</sub> ( $\mu\text{mol L}^{-1} \text{d}^{-1}$ )	PO <sub>4</sub> ( $\mu\text{mol L}^{-1} \text{d}^{-1}$ )
3	0	1.20	0.21	0.466	0.08	1.71	0	0
3	25	1.88	0.11	0.588	0.04	2.11	0	0.70
3	50	0.29	0.01	0.209	0.00	0.91	0.33	1.48
7	0	2.49	0.44	0.63	0.20	2.60	0	0
7	25	2.71	0.22	3.79	2.45	0.47	0	0.45
7	50	0.53	0.24	0.33	0.36	1.08	0	0.97
10	0	1.48	0.12	0.74	0.15	1.33	0	0
10	25	0.31	0.01	0.29	0.07	0.73	0	0
10	50	0.16	0	0.07	0.07	1.40	0	0

4 A near-Redfield stoichiometry in POC:PON indicates that the particulate organic matter (POM) is freshly derived from an  
 5 ongoing phytoplankton bloom, as phytoplankton generally assimilate carbon and nitrogen in relatively consistent proportions  
 6 during active growth. In contrast, deviations from the Redfield ratio (e.g., elevated C:N or C:P) typically indicate microbial  
 7 degradation and preferential remineralization of nitrogen and phosphorus (Redfield 1934; Geider and La Roche 2002; Sterner  
 8 and Elser 2017). The absence of NO<sub>x</sub> and the observed low N:P ratios suggest that nitrogen from earlier bloom phases has  
 9 been largely depleted, potentially creating a niche for N<sub>2</sub> fixation as a supplementary nitrogen source. The onset and  
 10 development of the bloom would be expected to lead to high nitrogen demands and intense competition for nitrogen sources.  
 11 Notably, despite the apparent balance in the POM pool, the N:P ratio indicates strong nitrogen depletion and nutrient exhaustion  
 12 within the ecosystem. This deficiency can be partly alleviated by N<sub>2</sub> fixation, providing possibly increasing amounts of nitrogen  
 13

**Deleted:** Consequently, it is possible that nutrients and Fe from the Isbræ glacier introduced into the Qeqertarsuaq are promoting a bloom and further provide a niche for diazotrophs to thrive (Arrigo et al. (2017)).

**Deleted:** compunds

**Deleted:** 3

**Formatted:** Line spacing: Multiple 1,46 li

**Deleted:** bloom. However, the absence of NO<sub>x</sub> (with the exception of one station) and the observed low N:P ratios suggest that any available nitrogen from earlier phases of the bloom has likely been depleted. This could create a niche for N<sub>2</sub> fixation as a supplementary nitrogen source, potentially supporting continued production during this stage of the bloom.

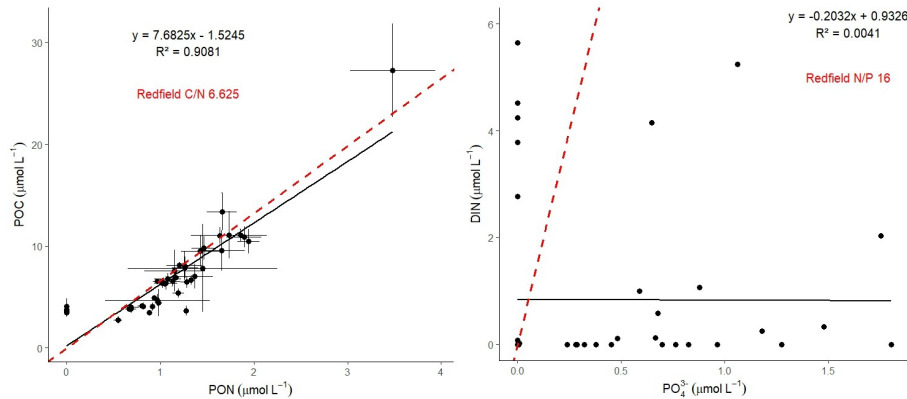
17 over the course of the bloom. Moreover, DIP is generally limited in the environment (Table 1); however, some organisms may  
18 still access it through luxury phosphorus uptake, storing excess phosphate when it is sporadically available. A recent study  
19 by Laso Perez et al. (2024) documented changes in microbial community composition during an Arctic bloom, focusing on  
20 nitrogen cycling. They observed a shift from chemolithotrophic to heterotrophic organisms throughout the summer bloom and  
21 noted increased activity to compete for various nitrogen sources. However, no *nifH* gene copies, indicative of nitrogen-fixing  
22 organisms, were found in their dataset based on metagenome-assembled genomes (MAGs). This is not unexpected due to the  
23 classically low abundance of diazotrophs in marine microbial communities which has often been described (Turk-Kubo et al.,  
24 2015; Farnelid et al., 2019). Given the high productivity and metabolic activity observed in Qeqertarsuaq during a similar  
25 bloom period, the detected diazotrophs (Section 3.3) may play a more significant role than previously thought. Across the 10  
26 stations there is considerable variability in POC and PON concentrations (Fig. 3). PON concentrations range from 0.0  $\mu\text{mol N}$   
27  $\text{L}^{-1}$  to 3.48  $\mu\text{mol N L}^{-1}$  (n=124), while POC concentrations range from 2.7  $\mu\text{mol C L}^{-1}$  to 27.2  $\mu\text{mol C L}^{-1}$  (n=144). The highest  
28 concentrations for both PON and POC were observed at station 7 at a depth of 25 m and coincide with the highest reported  $\text{N}_2$   
29 fixation rate (Figure Appendix A2 & A3). Generally, POC and PON concentrations decrease with depth, peaking at the deep  
30 chl *a* maximum (DCM), identified between 15 to 30 m across all stations. The DCM was identified based on measured chl *a*  
31 concentrations and previous descriptions in the region (Fox and Walker, 2022; Jensen et al., 1999). The variability in chl *a*  
32 concentrations indicates differences in phytoplankton abundance among the stations, with concentrations ranging between 0 to  
33 0.42  $\text{mg m}^{-3}$ . Excluding station 7, which exhibited the highest chl *a* concentration at the DCM (1.51  $\text{mg m}^{-3}$ ). While Tang et  
34 al. (2019) found that  $\text{N}_2$  fixation measurements strongly correlated to satellite estimates of chl *a* concentrations, our results did  
35 not show a statistically significant correlation between nitrogen fixation rates and chl *a* concentrations overall (Figures A2 &  
36 A3). However, as noted, Station 7 at 25 m represents a unique case. The elevated concentration of chl *a* at this station likely  
37 resulted from a local phytoplankton bloom induced by meltwater outflow from the Isbræ glacier and sea ice melting, which  
38 may help explain the observed nitrogen fixation rates (Arrigo et al., 2017; Wang et al., 2014). This study's findings are in  
39 agreement with prior reports of analogous blooms occurring in the region (Fox and Walker, 2022; Jensen et al., 1999).

Deleted: ¶

Field Code Changed

Deleted: ¶

i2



i3  
i4 **Figure 3.** The POC/PON and DIN/DIP ratios at all 10 stations. The red line represents the Redfield ratios of POC/PON (106:16) and DIN/DIP (16:1).  
i5

### 3.3 Potential Contribution of UCYN-A to Nitrogen Fixation During a Diatom Bloom: Insights and Uncertainties

i6  
i7 In our metagenomic analysis, we filtered the *nifH*, *nifD*, *nifK* genes, which code for the nitrogenase enzyme responsible for  
i8 catalyzing N<sub>2</sub> fixation. We could identify sequences related to UCYN-A, which dominated the sequence pool of diazotrophs,  
i9 particularly in the upper water masses (0 to 5 m) (Fig. 4). UCYN-A, a unicellular cyanobacterial symbiont, has a cosmopolitan  
i10 distribution and is thought to substantially contribute to global N<sub>2</sub> fixation, as documented by (Martínez-Pérez et al., 2016;  
i11 Tang et al., 2019). This conclusion is based on our metagenomic analysis, in which we set a sequence identity threshold of  
i12 95% for both *nif* and photosystem genes. Notably, we only recovered sequences related to UCYN-A within our *nif* sequence  
i13 pool, suggesting its predominance among detected diazotrophs. However, metagenomic approaches may underestimate overall  
i14 diazotroph diversity, and we cannot fully exclude the presence of other, less abundant diazotrophs that may have been missed  
i15 using this method. While UCYN-A was primarily detected in surface waters, we also observed relatively high *nifK* values at  
i16 S3 100m, an unusual finding given that UCYN-A is typically constrained to the euphotic zone. Previous studies have  
i17 predominantly reported UCYN-A in surface waters; for instance Harding et al. (2018) and Shiozaki et al. (2017) detected  
i18 UCYN-A exclusively in the upper layers of the Arctic Ocean. Additionally, Shiozaki et al. (2020) found UCYN-A at depths  
i19 extending to the 0.1% light level but not below 66 m in the Chukchi Sea. The detection of UCYN-A at 100 m in our study  
i20 suggests that alternative mechanisms, such as particle association, vertical transport, or local environmental conditions, may

**Deleted:** stations there is considerable variability in POC and PON concentrations (Fig. 3). PON concentrations range from 0.5 µmol N L⁻¹ to 4.0 µmol N L⁻¹ (n=124), while POC concentrations range from 2.5 µmol C L⁻¹ to 32.6 µmol C L⁻¹ (n=144). The highest concentrations for both PON and POC were observed at station 7 at a depth of 25 m and coincide with the highest reported N<sub>2</sub> fixation rate (Figure Appendix A2 & A3). Generally, POC and PON concentrations decrease with depth, peaking at the deep chl *a* maximum (DCM), identified between 15 to 30 m across all stations. The variability in chl *a* concentrations indicates differences in phytoplankton abundance among the stations, with concentrations ranging between 0 to 0.42 mg m⁻³. Excluding station 7, which exhibited the highest chl *a* concentration at the DCM (1.51 mg m⁻³). Tang et al. (2019) have found that N<sub>2</sub> fixation measurements strongly correlated to satellite estimates of chl *a* concentrations and thus may be an explanation for the presented N<sub>2</sub> fixation rates. The elevated concentration of chl *a* likely result from a local phytoplankton bloom induced by meltwater outflow from the Isbrae glacier and sea ice melting (Arrigo et al., 2017; Wang et al., 2014). This can also be seen<sup>†</sup>

**Deleted:** from satellite images (Appendix A1). This study's findings are in agreement with prior reports of analogous blooms occurring in the region (Fox and Walker, 2022; Jensen et al., 1999).<sup>†</sup>

UCYN

**Deleted:** -A might contribute to N<sub>2</sub> fixation during a diatom bloom...

3 facilitate its presence at depth. Interestingly, despite very low *niH* copy numbers being reported in nearby Baffin Bay by  
4 Robicheau et al. (2023), UCYN-A dominated the metagenomic *niH* community in our study, further underscoring this  
5 organisms's presence in Arctic surface coastal areas under certain environmental conditions. This warrants further  
6 investigation into the environmental drivers and potential processes enabling its occurrence in Arctic waters.

Formatted: Font: Italic

7 Due to the lack of genes such as those encoding Photosystem II and Rubisco, UCYN-A plays a significant role within the host  
8 cell and participates in fundamental cellular processes. Consequently it has evolved to become a closely integrated component  
9 of the host cell. Very recent findings demonstrate that UCYN-A imports proteins encoded by the host genome and has been  
10 described as an early form of N<sub>2</sub> fixing organelle termed a "Nitroplast" (Coale et al. (2024)).

11 Previous investigations document that they are critical for primary production, supplying up to 85% of the fixed nitrogen to their  
12 haptophyte host (Martínez-Pérez et al. (2016)). In addition to its high contribution to primary production, studies have shown  
13 that UCYN-A in high latitude waters fix similar amounts of N<sub>2</sub> per cell as in the tropical Atlantic Ocean, even in nitrogen-  
14 replete waters (Harding et al., 2018; Shiozaki et al., 2020; Martínez-Pérez et al., 2016; Krupke et al., 2015; Mills et al., 2020).  
15 However, estimating their contribution to N<sub>2</sub> fixation in our study is challenging, particularly since we detected cyanobacteria  
16 only at the surface but observe significant N<sub>2</sub> fixation rates below 5 m. The diazotrophic community is often underrepresented  
17 in metagenomic datasets due to the low abundance of nitrogenase gene copies, implying our data does not present a complete  
18 picture. We suspect a more diverse diazotrophic community exists, with UCYN-A being a significant contributor to N<sub>2</sub> fixation  
19 in Arctic waters. However, the exact proportion of its contribution requires further investigation.

Deleted: may

20 The contribution of N<sub>2</sub> fixation to carbon fixation (as percent of PP) is relatively low, at the time of our study. We identified  
21 genes such as *rbcL*, which encodes Rubisco, a key enzyme in the carbon fixation pathway and *psbA*, a gene encoding  
22 Photosystem II, involved in light-driven electron transfer in photosynthesis, in our metagenomic dataset. The gene *rbcL* (for the  
23 carbon fixation pathway) and the gene *psbA* (for primary producers) were used to track the community of photosynthetic primary  
24 producers in our metagenomic dataset. At station 7, elevated carbon fixation rates are correlated with high diatom  
25 (*Bacillariophyta*) abundance and increased chl *a* concentration (Fig. 4), suggesting the onset of a bloom, which is also  
26 observable via satellite images (Appendix A1). We hypothesize that meltwater, carrying elevated nutrient and trace metal  
27 concentrations, was rapidly transported away from the glacier through the Vaigat Strait by strong winds, leading to increased  
28 productivity, as previously described by Fox and Walker (2022) & Jensen et al. (1999). The elevated diatom abundance and  
29 primary production rates at station 7 coincide with the highest N<sub>2</sub> fixation rates, which could possibly point toward a possible  
30 diatom-diazotroph symbiosis (Foster et al., 2022, 2011; Schvarcz et al., 2022). However, we did not detect a clear diazotrophic  
31 signal directly associated with the diatoms in our metagenomic dataset, which might be due to generally underrepresentation of  
32 diazotrophs in metagenomes due to low abundance or low sequencing coverage. To investigate this further, we examined  
33 the taxonomic composition of *Bacillariophyta* at higher resolution. Among the various abundant diatom genera,  
34 *Rhizosolenia* and *Chaetoceros* have been identified as symbiosis with diazotrophs (Grosse, et al., 2010; Foster, et al.,  
35 2010), representing less than 6% or 15% of *Bacillariophyta*, based on *rbcL* or *psbA*, respectively (Figure Appendix A4).  
36 Although we underestimate diazotrophs to an extent, the presence of certain diatom-diazotroph symbiosis could help

Deleted: but may increase with a further onset of bloom periods. ....

Formatted: Indent: Left: 0 cm

Deleted: s

Deleted: However,

Deleted: ny relevant

Deleted: group

Deleted: observed

Deleted: their absence or due to the

Deleted: .

Formatted: Font: Italic

Formatted: Font: Italic

Formatted: Font: Italic

Formatted: Font: Italic

7 explain the high nitrogen fixation rates in the diatom bloom to a certain degree. Compilation of *nif* sequences identified  
 8 from this study as well as homologous from their NCBI top hit were added in Table S1. However, we cannot tell if the  
 9 diazotrophs belong to UCYN-A1 or UCYN-A2, or UCYN-A3. Based on the Pierella Karlusich et al. (2021), they  
 10 generated clonal *nifH* sequences from Tara Oceans, which the length of *nifH* sequences is much shorter than the two  
 11 *nifH* sequences we generated in our study. Also, the available UCYN-A2 or UCYN-A3 *nifH* sequences from NCBI were  
 12 shorter than the two *nifH* sequences we generated. Therefore, it would be not accurate to assign the *nifH* sequences to  
 13 either group under UCYN-A. Furthermore, not much information is available regarding the different groups of UCYN-  
 14 A using marker genes of *nifD* and *nifK*.

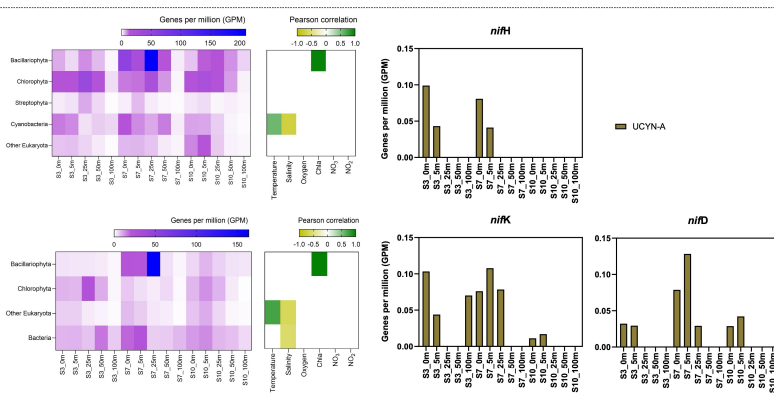
**Formatted:** Font: Italic

**Moved (insertion) [1]**

**Deleted:** Therefore, we can only assume that such a symbiosis explains the elevated rates. Additional molecular approaches would be necessary to enhance our understanding show a more detailed picture of the diazotrophic community.¶

**Moved up [1]:** a symbiosis explains the elevated rates. Additional molecular approaches would be necessary to enhance our understanding show a more detailed picture of the diazotrophic community.¶

**Deleted:** ¶



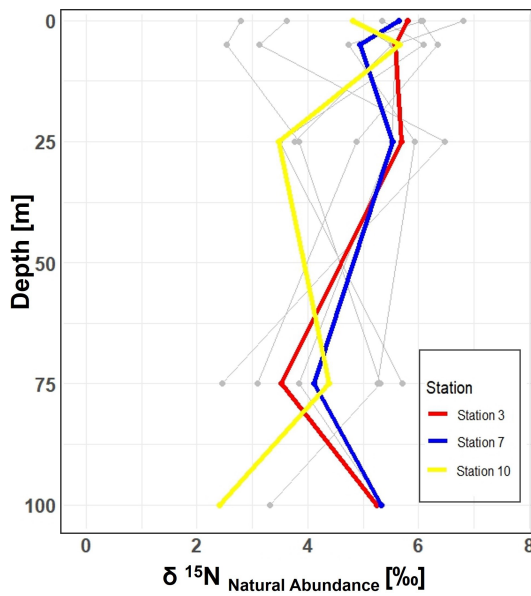
5  
 6  
 7  
 8  
 9 **Figure 4.** Upper left image: *psbA* with correlation plot. Lower left image: *rbcL* with correlation plot. Right image: *nifH*, *nifD*, *nifK* genes  
 0 per million reads in the metagenomic datasets. All figures display molecular data from metagenomic dataset for all sampled depth of station  
 1 3,7,10

2  
 3 There is evidence that UCYN-A have a higher Fe demand, with input through meltwater or river runoff potentially being  
 4 advantageous to those organisms (Shiozaki et al., 2017, 2018; Cheung et al., 2022). Consequently, UCYN-A might play a  
 5 more critical role in the future with increased Fe-rich meltwater runoff. UCYN-A can potentially fuel primary productivity by  
 6 supplying nitrogen, especially with increased melting, nutrient inputs, and more light availability due to rising temperatures as-  
 7 sociated with climate change. This predicted enhancement of primary productivity may contribute to the biological drawdown  
 8 of CO<sub>2</sub>, acting as a negative feedback mechanism. These projections are based on studies forecasting increased temperatures,  
 9 melting, and resulting biogeochemical changes leading to higher primary productivity. However large uncertainties make pre-  
 10 dictions very difficult and should be handled with care. Thus we can only hypothesize that UCYN-A might be coupled to these

11 dynamics by providing essential nitrogen.

### 12 3.4 $\delta^{15}\text{N}$ Signatures in particulate organic nitrogen show no clear evidence of nitrogen fixation

13  
14 Stable isotopic composition, expressed using the  $\delta^{15}\text{N}$  notation, serve as indicators for understanding nitrogen dynamics  
15 because different biogeochemical processes fractionate nitrogen isotopes in distinct ways (Montoya (2008)). However, it is  
16 important to keep in mind that the final isotopic signal is a combination of all processes and an accurate distinction between  
17 processes cannot be made.  $\text{N}_2$  fixation tends to enrich nitrogenous compounds with lighter isotopes, producing OM with  
18 isotopic values ranging approximately from -2 to +2 ‰ (Dähnke and Thamdrup (2013)). Upon complete remineralization and  
19 oxidation, organic matter contributes to a reduction in the average  $\delta$ -values in the open ocean (e.g. Montoya et al. (2002);  
20 Emeis et al. (2010)). Whereas processes like denitrification and anammox preferentially remove lighter isotopes, leading to  
21 enrichment in heavier isotopes and delta values up to -25 ‰.



13  
14  
15 **Figure 5.** Vertical profiles of  $\delta^{15}\text{N}$  natural abundance signatures in PON across 10 stations in the study area. Incubation stations 3, 7, and 10  
16 are highlighted in red, blue, and yellow, respectively. The figure shows variations in  $\delta^{15}\text{N}$  signatures with depth at each station, providing

17 insight into nitrogen cycling in the study area.

18 Thus,  $\delta^{15}\text{N}$  values help to identify different processes of the nitrogen cycle generally present in a system (Dähnke and Tham-  
19 drup (2013)). In our study, the  $\delta^{15}\text{N}$  values of PON from all 10 stations, range between 2.45‰ and 8.30‰ within the 0 to  
0 100 m depth range, thus do not exhibit a clear signal indicative of  $\text{N}_2$  fixation. This suggests that  $\text{N}_2$  fixation ~~may~~ contributes  
1 only a certain fraction to export production or that it ~~might have begun~~, to play a role in, isotopic fractionation ~~during later~~  
2 stages of the bloom. However, due to the limited temporal resolution and lack of direct measurements of N sources over time,  
3 we cannot confirm this dynamic. Additional data – including time-series isotopic profiles and turnover measurements of  
4 subsurface nitrate and diazotroph activity – would be needed to establish a causal link between  $\text{N}_2$  fixation and the observed  
5 isotopic patterns in the bloom context. The composition of OM in the surface ocean is influenced by the nitrogen substrate and  
6 the fractionation factor during photosynthesis. When nitrate is depleted in the surface ocean, the isotopic signature of OM  
7 produced during photosynthesis will mirror that of the nitrogen substrate. This substrate can originate from either nitrate in the  
8 subsurface or  $\text{N}_2$  fixation. Notably, nitrate, the primary form of dissolved nitrogen in the open ocean, typically exhibits an  
9 average stable isotope value of around  
10

11 5‰. No fractionation occurs during photosynthesis because the nitrogen source is entirely taken up in the surface waters  
12 (Sigman et al. (2009)). In Qeqertarsuaq, where similar conditions prevail, this suggests that factors other than  $\text{N}_2$  fixation ~~are~~  
13 influencing the observed  $\delta$ -values and POM is sustained by nitrogen sources from deeper subsurface waters, as observed in  
14 earlier studies (Fox and Walker (2022)).

15 In the eastern Baffin Bay waters, Atlantic water masses serve as an important source of nitrate for sustaining primary produc-  
16 tivity, which is also reflected in the nitrogen isotopic signature in this study (Sherwood et al. (2021)). The influx of Atlantic  
17 waters, characterized by  $\text{NO}_3^-$  values of approximately 5‰, closely matches the  $\delta^{15}\text{N}$  values of observed PON concentrations  
18 in our study. This suggests that Atlantic-derived  $\text{NO}_3^-$  serves as a primary source of new nitrogen to the initial stages of bloom  
19 development (Fox and Walker, 2022; Knies, 2022). The mechanisms through which subsurface nitrate reaches the euphotic  
0 layer are not well understood. However, potential pathways include vertical migration of phytoplankton and physical mixing.  
1 Subsequently, nitrogen undergoes rapid recycling and remineralization processes to meet the system's nitrogen demands  
2 (Jensen et al. (1999)).

#### 3 4 Conclusion

4 Our study highlights the occurrence of elevated rates of  $\text{N}_2$  fixation in Arctic coastal waters, particularly prominent at station 7,  
5 where they coincide with high chl  $a$  values, indicative of heightened productivity. Satellite observations tracing the origin of a  
6 bloom near the Isbræ Glacier, subsequently moving through the Vaigat strait, suggest a recurring phenomenon likely triggered  
7 by increased nutrient-rich meltwater originating from the glacier. This aligns with previous reports by Jensen et al. (1999) &  
8 Fox and Walker (2022), underlining the significance of such events in driving primary productivity in the region. The contribu-  
9 tion of  $\text{N}_2$  fixation to primary production was low (average 1.57 %) across the stations. Since the demand was high relative to  
10

**Deleted:** likely

**Deleted:** only started

**Deleted:** contribute

**Deleted:** to

**Deleted:** e

**Deleted:** in

**Deleted:** dynamic

**Deleted:** -

**Deleted:** may

**Deleted:** be

**Deleted:** As the bloom progresses and nitrogen from  
Atlantic waters is depleted,  $\text{N}_2$  fixation may provide an  
additional nitrogen source, supporting continued primary  
productivity. ...

the new nitrogen provided by N<sub>2</sub> fixation, the observed primary production must be sustained by the already present or adequate amount of subsurface supply of NO<sub>x</sub> nutrients in the seawater. This is also visible in the isotopic signature of the POM (Fox and Walker, 2022; Sherwood et al., 2021). However, the detected N<sub>2</sub> fixation rates are likely linked to the development of the fresh secondary summer bloom, which could be sustained by high nutrient and Fe availability from melting, potentially leading the system into a nutrient-limited state. The ongoing high demand for nitrogen compounds may suggest an onset to further sustain the bloom, but it remains speculative whether Fe availability definitively contributes to this process. The occurrence of such double blooms has increased by 10 % in the Qeqertarsuaq and even 33 % in the Baffin Bay, with further projected increases moving north from Greenland (Kalaallit Nunaat) waters (Ardyna et al. (2014)). Thus, nutrient demands are likely to increase, and the role of N<sub>2</sub> fixation can become more significant. The diazotrophic community in this study is dominated by UCYN-A in surface waters and may be linked to diatom abundance in deeper layers. This co-occurrence of diatoms and N<sub>2</sub> fixers in the same location is probably due to the co-limitation of similar nutrients, rather than a symbiotic relationship. Thus, this highlights the significant presence of diazotrophs despite their limited representation in datasets. It also highlights the potential for further discoveries, as existing datasets likely underestimate the full extent of the diazotrophic community (Laso Perez et al., 2024; Shao et al., 2023; Shiozaki et al., 2017, 2023). The reported N<sub>2</sub> fixation rates in the Vaigat strait within the Arctic Ocean are notably higher than those observed in many other oceanic regions, emphasizing that N<sub>2</sub> fixation is an active and significant process in these high-latitude waters. When compared to measured rates across various ocean systems using the <sup>15</sup>N approach, the significance of these findings becomes clear. For instance, N<sub>2</sub> fixation rates are sometimes below the detection limit and often relatively low ranging from 0.8 to 4.4 nmol N L<sup>-1</sup> d<sup>-1</sup> (Löscher et al., 2020, 2016; Turk et al., 2011). In contrast, higher rates reach up to 20 nmol N L<sup>-1</sup> d<sup>-1</sup> (Rees et al. (2009)) and sometime exceptional high rates range from 38 to 610 nmol N L<sup>-1</sup> d<sup>-1</sup> (Bonnet et al. (2009)). The Arctic Ocean rates are thus significant in the global context, underscoring the region's role in the global nitrogen cycle and the importance of N<sub>2</sub> fixation in supporting primary productivity in these waters.

These findings highlight the urgent need to understand the interplay between seasonal variations, sea-ice dynamics, and hydrographic conditions in Qeqertarsuaq. As climate change accelerates the melting of the Greenland Ice Sheet at Jakobshavn Isbræ, shifts in hydrodynamic patterns and hydrographic conditions in Qeqertarsuaq are anticipated. The resulting influx of warmer waters could significantly reshape the bay's hydrography, making it crucial to comprehend the coupling of climate-driven changes and oceanic processes in this vital Arctic region. Our study provides key insights into these dynamics and underscores the importance of continued investigation to predict Qeqertarsuaq's future hydrographic state. By detailing the environmental and hydrographic changes, we contribute valuable knowledge to the broader context of N<sub>2</sub> fixation in the Arctic Ocean. Given nitrogen's pivotal role in Arctic ecosystem productivity, it is essential to explore diazotrophs, quantify N<sub>2</sub> fixation, and assess their impact on ecosystem services as climate change progresses.

Deleted: may

Field Code Changed  
Deleted: ?;

## Appendix A

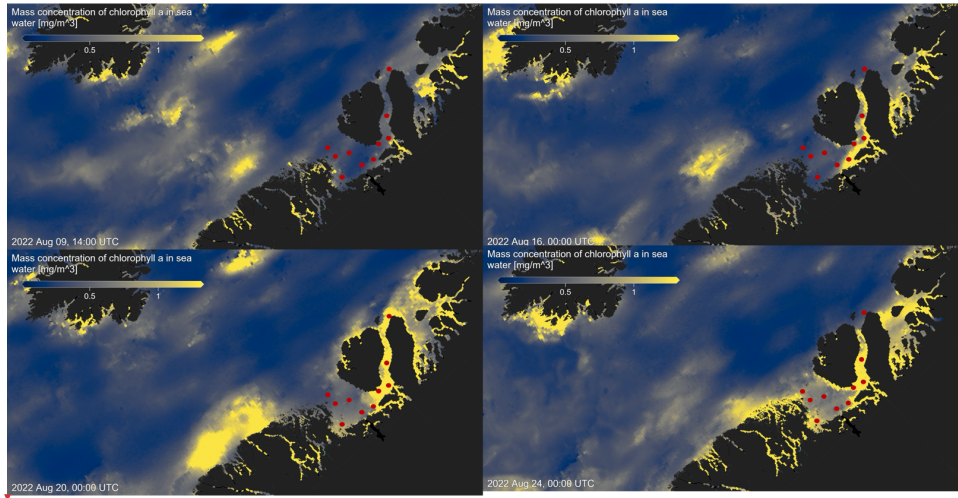
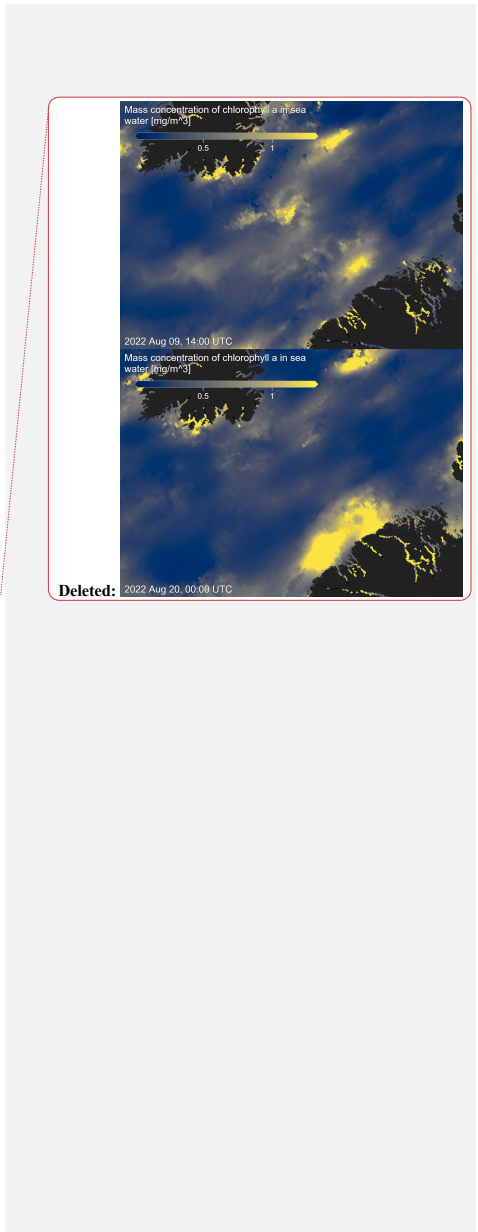
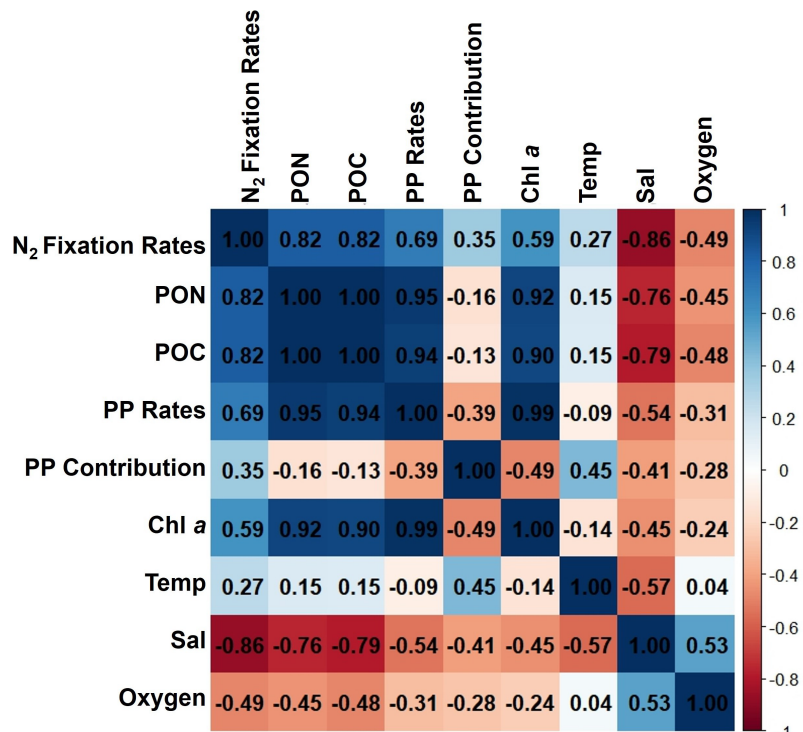
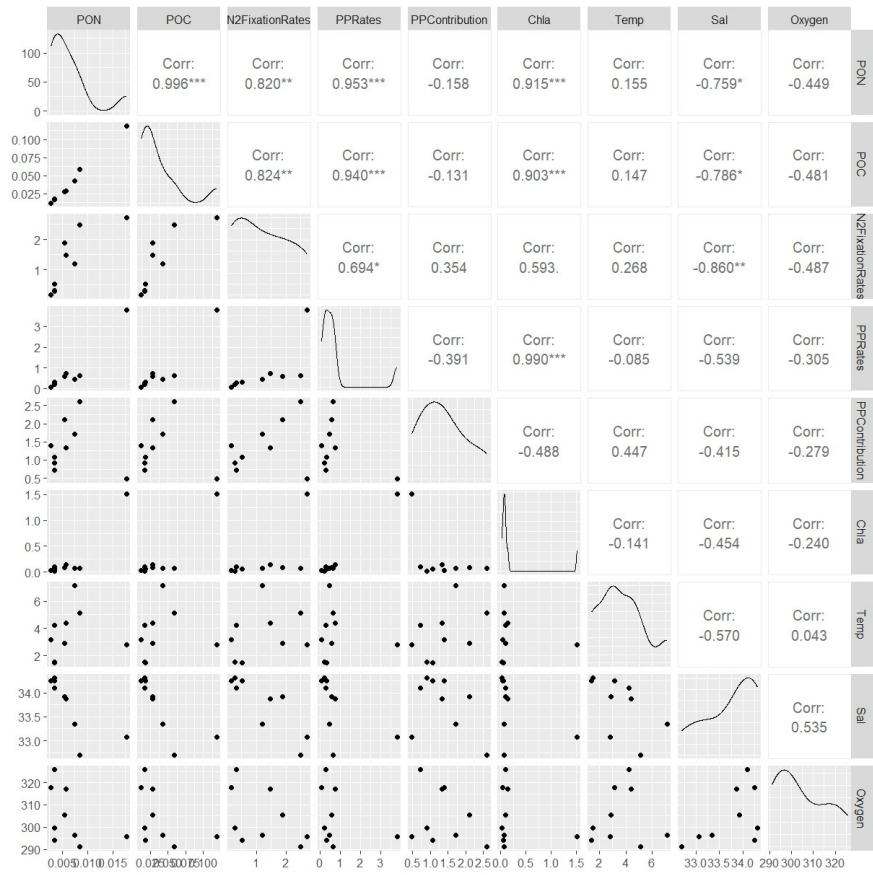


Figure A1. Chlorophyll *a* concentration  $\text{mg m}^{-3}$  at four time points before, during, and after sea water sampling in August 2022 (sampling stations indicated by red dots), obtained from MODIS-Aqua; <https://giovanni.gsfc.nasa.gov> (Aqua MODIS Global Mapped Chl *a* Data, version R2022.0, DOI:10.5067/AQUA/MODIS/L3M/CHL/2022), 4 km resolution, last access 03 June 2024





16  
17  
18 **Figure A2.** Correlation matrix of environmental and biological variables. The plot shows the correlation coefficients between the following  
19 parameters: N<sub>2</sub> fixation rates, PON, POC, PP rates, the contribution N<sub>2</sub> fixation to PP (PP contribution), Chl a, temperature (Temp),  
20 salinity (Sal), and Oxygen. The scale ranges from -1 to 1, where values close to 1 or -1 indicate strong positive or negative correlations, respectively,  
21 and values near 0 indicate weak or no correlation. The color intensity represents the strength and direction of the correlations, facilitating the  
22 identification of relationships among the variables



13  
14  
15 **Figure A3.** This figure displays a ggpairs plot, showing pairwise relationships and correlations between biological and environmental vari-  
16 ables. Pearson correlation coefficients displayed in the upper triangular panel, indicating the strength and significance of linear relationships.  
17 Statistical significance levels are indicated by stars (\*), where \* indicates  $p < 0.05$ , \*\* indicates  $p < 0.01$  and \*\*\* indicates  $p < 0.001$

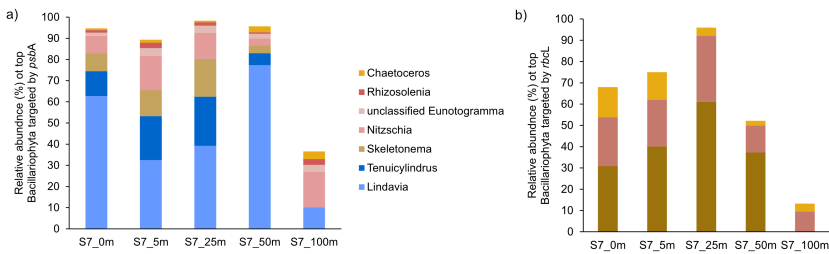


Figure A4: Taxonomic composition of Bacillariophyta at Station 7 based on a) psbA and b) rbcL marker genes. The figure shows the relative abundance of Bacillariophyta genera detected in the metagenomic dataset, grouped by gene-specific classifications.

Station	Parameter (X)	Value	SD	$\delta\text{NFR}/\delta X$	Error contribution ( $(SD \times  \delta\text{NFR}/\delta X )^2$ )	% Total error	Summary (nmol N L <sup>-1</sup> d <sup>-1</sup> )
3	$\Delta t$	1.00	0.00	0.00	0.00	0.00	Mean = 1.13 LOD = 0.73 MQR = 0.12
	$A_{N2}$	3.92%	0.00	0.00	0.00	0.00	
	$A_{PNO}$	0.370%	4.24 x 10 <sup>-6</sup>	2.63 x 10 <sup>6</sup>	2.46 x 10 <sup>2</sup>	29.49	
	$A_{PNf}$	0.420%	3.7 x 10 <sup>-5</sup>	2.36 x 10 <sup>5</sup>	3.03 x 10 <sup>2</sup>	35.54	
	$[PN]_t$	1.69 x 10 <sup>3</sup>	1.24 x 10 <sup>3</sup>	5.12 x 10 <sup>-2</sup>	3.21 x 10 <sup>2</sup>	34.97	
7	$\Delta t$	1.00	0.00	0.00	0.00	0.00	Mean = 1.92 LOD = 1.91 MQR = 0.47
	$A_{N2}$	3.92%	0.00	0.00	0.00	0.00	
	$A_{PNO}$	0.369%	4.0 x 10 <sup>-7</sup>	1.57 x 10 <sup>7</sup>	2.06 x 10 <sup>3</sup>	25.17	

			$10^{-6}$				
	<u>Apnf</u>	<u>0.407%</u>	<u>5.47</u> <u><math>\times 10^{-5}</math></u>	<u><math>9.25 \times 10^5</math></u>	<u><math>2.79 \times 10^3</math></u>	<u>36.88</u>	
	<u>[PN]t</u>	<u>4.62 x</u> <u><math>10^3</math></u>	<u>8.2 x</u> <u><math>10^2</math></u>	<u><math>6.77 \times 10^{-2}</math></u>	<u><math>2.87 \times 10^3</math></u>	<u>37.95</u>	
10	<u>At</u>	<u>1.00</u>	<u>0.00</u>	<u>0.00</u>	<u>0.00</u>	<u>0.00</u>	<u>Mean =</u> <u>0.90</u> <u>LOD =</u> <u>0.96</u> <u>MQR =</u> <u>0.06</u>
	<u>AN2</u>	<u>3.92%</u>	<u>0.00</u>	<u>0.00</u>	<u>0.00</u>	<u>0.00</u>	
	<u>Apno</u>	<u>0.371%</u>	<u>1.89</u> <u><math>\times 10^{-6}</math></u>	<u>-2.01 x</u> <u><math>10^2</math></u>	<u><math>1.44 \times 10^{-3}</math></u>	<u>31.24</u>	
	<u>Apnf</u>	<u>0.371%</u>	<u>2.22</u> <u><math>\times 10^{-6}</math></u>	<u><math>2.01 \times 10^2</math></u>	<u><math>2.05 \times 10^{-3}</math></u>	<u>34.85</u>	
	<u>[PN]t</u>	<u>5.91 x</u> <u><math>10^2</math></u>	<u>1.89</u> <u><math>\times 10^3</math></u>	<u><math>-1.56 \times 10^{-4}</math></u>	<u><math>3.69 \times 10^{-3}</math></u>	<u>33.91</u>	

Formatted: Keep with next

Formatted: Caption

6 *Appendix Table 1: Sensitivity analysis for  $N_2$  fixation rates. The contribution of each source of error to the total uncertainty was determined and*  
7 *calculated after Montoya et al., (1996). Average values and standard deviations (SD) are provided for all parameters at each station. The partial*  
8 *derivative ( $\partial NFR / \partial X$ ) of the  $N_2$  fixation rate measurements is calculated for each parameter and evaluated using the provided average and*  
9 *standard deviation. The total and relative error are given for each parameter. Mean represents the average  $N_2$  fixation rate measurement. MOR*  
10 *(minimal quantifiable rate) represents the total uncertainty linked to every measurement and is calculated using standard propagation of error.*  
11 *LOD (limit of detection) represents an alternative detection limit defined as  $\Delta APN = 0.00146$ .*

12 *Data availability.* The presented data collected during the cruise will be made accessible on PANGEA. The molecular datasets have been  
13 deposited with the accession number: Bioproject PRJNA1133027.

Deleted: Bioproject PRJNA1133027.

14 *Author contributions.* IS carried out fieldwork and laboratory work at the University of Southern Denmark, and wrote the majority of the  
15 manuscript. ELP, AM, and EL conducted fieldwork and laboratory work at the University of Southern Denmark. PX performed metagenomic  
16 analysis and created the corresponding graphs. CRL designed the study, provided supervision and guidance throughout the project, and  
17 contributed to the writing and revision of the manuscript. All authors contributed to the conception of the study and participated in the writing  
18 and revision of the manuscript.

19 *Competing interests.* The authors declare that they have no known competing financial interests or personal relationships that could have  
20 appeared to influence the work reported in this paper. One of the authors, CRL, serves as an Associate Editor for Biogeosciences.

|2 *Acknowledgements.* This work was supported by the Velux Foundation (grant no.29411 to Carolin R. Löscher) and through the DFF grant  
|3 from the the Independent Research Fund Denmark (grant no. 0217-00089B to Lasse Riemann, Carolin R. Löscher and Stiig Markager). ELP  
|4 was supported by a postdoctoral contract from Danmarks Frie Forskningsfond (DFF, 1026-00428B) at SDU, and by a Marie Skłodowska-  
|5 Curie postdoctoral fellowship (HORIZON291 MSCA-2021-PF-01, project number: 101066750) by the European Commission at Princeton  
|6 University. We sincerely thank the captain and crew of the P540 during the cruise on the Danish military vessel for their invaluable support and  
|7 cooperation at sea. Our gratitude extends to Isaaffik Arctic Gateway for providing the infrastructure and opportunities that made this project  
|8 possible. We also acknowledge Zarah Kofoed for her technical support in the laboratory and thank all the Nordceee laboratory technicians for  
|9 their general assistance.

## |0 **References**

|1 Ardyna, M. and Arrigo, K. R.: Phytoplankton dynamics in a changing Arctic Ocean, *Nature Climate Change*, 10, 892–903, 2020.  
|2 Ardyna, M., Babin, M., Gosselin, M., Devred, E., Rainville, L., and Tremblay, J.-É.: Recent Arctic Ocean sea ice loss triggers novel fall  
|3 phytoplankton blooms, *Geophysical Research Letters*, 41, 6207–6212, 2014.  
|4 Arrigo, K. R. and van Dijken, G. L.: Continued increases in Arctic Ocean primary production, *Progress in oceanography*, 136, 60–70, 2015.  
|5 Arrigo, K. R., van Dijken, G., and Pabi, S.: Impact of a shrinking Arctic ice cover on marine primary production, *Geophysical Research  
|6 Letters*, 35, 2008.  
|7 Arrigo, K. R., van Dijken, G. L., Castelao, R. M., Luo, H., Rennermalm, Å. K., Tedesco, M., Mote, T. L., Oliver, H., and Yager, P. L.:  
|8 Melting glaciers stimulate large summer phytoplankton blooms in southwest Greenland waters, *Geophysical Research Letters*, 44, 6278–  
|9 6285, 2017.  
|10 Bhatia, M. P., Kujawinski, E. B., Das, S. B., Breier, C. F., Henderson, P. B., and Charette, M. A.: Greenland meltwater as a significant and  
|11 potentially bioavailable source of iron to the ocean, *Nature Geoscience*, 6, 274–278, 2013.  
|12 Blais, M., Tremblay, J.-É., Jungblut, A. D., Gagnon, J., Martin, J., Thaler, M., and Lovejoy, C.: Nitrogen fixation and identification of  
|13 potential diazotrophs in the Canadian Arctic, *Global Biogeochemical Cycles*, 26, 2012.  
|14 Bonnet, S., Biegala, I. C., Dutrieux, P., Slemmons, L. O., and Capone, D. G.: Nitrogen fixation in the western equatorial Pacific: Rates,  
|15 diazotrophic cyanobacterial size class distribution, and biogeochemical significance, *Global Biogeochemical Cycles*, 23, 2009.  
|16 Buchanan, P. J., Chase, Z., Matear, R. J., Phipps, S. J., and Bindoff, N. L.: Marine nitrogen fixers mediate a low latitude pathway for  
|17 atmospheric CO<sub>2</sub> drawdown, *Nature Communications*, 10, 4611, 2019.  
|18 Cantalapiedra, C. P., Hernández-Plaza, A., Letunic, I., Bork, P., and Huerta-Cepas, J.: eggNOG-mapper v2: functional annotation, orthology  
|19 assignments, and domain prediction at the metagenomic scale, *Molecular biology and evolution*, 38, 5825–5829, 2021.  
|20 Capone, D. G. and Carpenter, E. J.: Nitrogen fixation in the marine environment, *Science*, 217, 1140–1142, 1982.  
|21 Chen, Y., Chen, Y., Shi, C., Huang, Z., Zhang, Y., Li, S., Li, Y., Ye, J., Yu, C., Li, Z., et al.: SOAPnuke: a MapReduce acceleration-supported  
|22 software for integrated quality control and preprocessing of high-throughput sequencing data, *Gigascience*, 7, gix120, 2018.  
|23 Cheung, S., Liu, K., Turk-Kubo, K. A., Nishioka, J., Suzuki, K., Landry, M. R., Zehr, J. P., Leung, S., Deng, L., and Liu, H.: High biomass  
|24 turnover rates of endosymbiotic nitrogen-fixing cyanobacteria in the western Bering Sea, *Limnology and Oceanography Letters*, 7, 501–  
|25 509, 2022.  
|26 Coale, T. H., Loconte, V., Turk-Kubo, K. A., Vanslembrouck, B., Mak, W. K. E., Cheung, S., Ekman, A., Chen, J.-H., Hagino, K., Takano,  
|27 Y., et al.: Nitrogen-fixing organelle in a marine alga, *Science*, 384, 217–222, 2024.  
|28 Dähnke, K. and Thamdrup, B.: Nitrogen isotope dynamics and fractionation during sedimentary denitrification in Boknafjord, Baltic Sea,

0 Biogeosciences, 10, 3079–3088, 2013.

1 Damm, E., Helmke, E., Thoms, S., Schauer, U., Nöthig, E., Bakker, K., and Kiene, R.: Methane production in aerobic oligotrophic surface

2 water in the central Arctic Ocean, Biogeosciences, 7, 1099–1108, 2010.

3 Diez, B., Bergman, B., Pedrós-Alió, C., Antó, M., and Snoeijs, P.: High cyanobacterial nifH gene diversity in Arctic seawater and sea ice

4 brine, Environmental microbiology reports, 4, 360–366, 2012.

5 Emeis, K.-C., Mara, P., Schlarbaum, T., Möbius, J., Dähnke, K., Struck, U., Mihalopoulos, N., and Krom, M.: External N inputs and internal

6 N cycling traced by isotope ratios of nitrate, dissolved reduced nitrogen, and particulate nitrogen in the eastern Mediterranean Sea, Journal

7 of Geophysical Research: Biogeosciences, 115, 2010.

8 Falkowski, P. G., Fenchel, T., and Delong, E. F.: The microbial engines that drive Earth's biogeochemical cycles, science, 320, 1034–1039,

9 2008.

10 Farnelid, H., Andersson, A. F., Bertilsson, S., Al-Soud, W. A., Hansen, L. H., Sørensen, S., Steward, G. F., Hagström, Å., and Riemann, L.:

11 Nitrogenase gene amplicons from global marine surface waters are dominated by genes of non-cyanobacteria, PLoS one, 6, e19 223, 2011.

12 Farnelid, H., Turk-Kubo, K., Ploug, H., Ossolinski, J. E., Collins, J. R., Van Mooy, B. A., and Zehr, J. P.: Diverse diazotrophs are present on

13 sinking particles in the North Pacific Subtropical Gyre, The ISME journal, 13, 170–182, 2019.

14 Fernández-Méndez, M., Turk-Kubo, K. A., Buttigieg, P. L., Rapp, J. Z., Krumpen, T., and Zehr, J. P.: Diazotroph diversity in the sea ice, melt

15 ponds, and surface waters of the Eurasian Basin of the Central Arctic Ocean, Frontiers in microbiology, 7, 217 140, 2016.

16 [Foster, R. A., Goebel, N. L., & Zehr, J. P.: Isolation of calothrix rhizosoleniae \(cyanobacteria\) strain SC01 from chaetoceros](#)

17 [\(bacillariophyta\) spp. diatoms of the subtropical north pacific ocean 1. Journal of Phycology, 46\(5\), 1028-1037, 2010.](#)

18 Foster, R. A., Kuypers, M. M., Vagner, T., Paerl, R. W., Musat, N., and Zehr, J. P.: Nitrogen fixation and transfer in open ocean diatom–

19 cyanobacterial symbioses, The ISME journal, 5, 1484–1493, 2011.

20 Foster, R. A., Tienken, D., Littmann, S., Whitehouse, M. J., Kuypers, M. M., and White, A. E.: The rate and fate of N2 and C fixation by

21 marine diatom-diazotroph symbioses, The ISME journal, 16, 477–487, 2022.

22 Fox, A. and Walker, B. D.: Sources and Cycling of Particulate Organic Matter in Baffin Bay: A Multi-Isotope  $\delta^{13}\text{C}$ ,  $\delta^{15}\text{N}$ , and  $\Delta^{14}\text{C}$

23 Approach, Frontiers in Marine Science, 9, 846 025, 2022.

24 Fu, L., Niu, B., Zhu, Z., Wu, S., and Cd-hit, W. L.: Accelerated for clustering the next-generation sequencing data, Bioinformatics, 28,

25 3150–3152, 2012.

26 Galloway, J., Dentener, F., Capone, D., Boyer, E., Howarth, R., Seitzinger, S., Asner, G., Cleveland, C., Green, P., Holland, E., et al.: Nitrogen

27 cycles: past, present, and future. Biogeochemistry 70, 153e226, 2004.

28 García-Robledo, E., Corzo, A., and Papaspyrou, S.: A fast and direct spectrophotometric method for the sequential determination of nitrate

29 and nitrite at low concentrations in small volumes, Marine Chemistry, 162, 30–36, 2014.

30 [Geider, R. J., & La Roche, J.: Redfield revisited: variability of C \[ratio\] N \[ratio\] P in marine microalgae and its biochemical](#)

31 [basis. European Journal of Phycology, 37\(1\), 1-17, 2002.](#)

32 Gladish, C. V., Holland, D. M., and Lee, C. M.: Oceanic boundary conditions for Jakobshavn Glacier. Part II: Provenance and sources of

33 variability of Disko Bay and Ilulissat icefjord waters, 1990–2011, Journal of Physical Oceanography, 45, 33–63, 2015.

34 [Grosse, J., Bombar, D., Doan, H. N., Nguyen, L. N., & Voss, M.: The Mekong River plume fuels nitrogen fixation and determines](#)

35 [phytoplankton species distribution in the South China Sea during low and high discharge season. Limnology and Oceanography, 55\(4\),](#)

36 [1668-1680, 2010.](#)

Formatted: English (UK)

Formatted: Indent: Left: 0,14 cm, First line: 0 cm

Formatted: Font: Not Italic

Formatted: Font: Not Italic

Formatted

7 Großkopf, T., Mohr, W., Baustian, T., Schunck, H., Gill, D., Kuypers, M. M., Lavik, G., Schmitz, R. A., Wallace, D. W., and LaRoche, J.:  
8 Doubling of marine dinitrogen-fixation rates based on direct measurements, *Nature*, 488, 361–364, 2012.

9 Gruber, N.: The dynamics of the marine nitrogen cycle and its influence on atmospheric CO<sub>2</sub> variations, in: *The ocean carbon cycle and*  
0 *climate*, pp. 97–148, Springer, 2004.

1 Gruber, N. and Galloway, J. N.: An Earth-system perspective of the global nitrogen cycle, *Nature*, 451, 293–296, 2008.

2 Gruber, N. and Sarmiento, J. L.: Global patterns of marine nitrogen fixation and denitrification, *Global biogeochemical cycles*, 11, 235–266,  
3 1997.

4 Haine, T. W., Curry, B., Gerdes, R., Hansen, E., Karcher, M., Lee, C., Rudels, B., Spreen, G., de Steur, L., Stewart, K. D., et al.: Arctic  
5 freshwater export: Status, mechanisms, and prospects, *Global and Planetary Change*, 125, 13–35, 2015.

6 Hanna, E., Huybrechts, P., Steffen, K., Cappelen, J., Huff, R., Shuman, C., Irvine-Fynn, T., Wise, S., and Griffiths, M.: Increased runoff from  
7 melt from the Greenland Ice Sheet: a response to global warming, *Journal of Climate*, 21, 331–341, 2008.

8 Hansen, M. O., Nielsen, T. G., Stedmon, C. A., and Munk, P.: Oceanographic regime shift during 1997 in Disko Bay, western Greenland,  
9 *Limnology and Oceanography*, 57, 634–644, 2012.

10 Harding, K., Turk-Kubo, K. A., Sipler, R. E., Mills, M. M., Bronk, D. A., and Zehr, J. P.: Symbiotic unicellular cyanobacteria fix nitrogen in  
11 the Arctic Ocean, *Proceedings of the National Academy of Sciences*, 115, 13 371–13 375, 2018.

12 Hawking, J., Wadham, J., Tranter, M., Lawson, E., Sole, A., Cowton, T., Tedstone, A., Bartholomew, I., Nienow, P., Chandler, D., et al.:  
13 The effect of warming climate on nutrient and solute export from the Greenland Ice Sheet, *Geochemical Perspectives Letters*, pp. 94–104,  
14 2015.

15 Hawking, J. R., Wadham, J. L., Tranter, M., Raiswell, R., Benning, L. G., Statham, P. J., Tedstone, A., Nienow, P., Lee, K., and Telling, J.:  
16 Ice sheets as a significant source of highly reactive nanoparticulate iron to the oceans, *Nature communications*, 5, 1–8, 2014.

17 Hendry, K. R., Huvenne, V. A., Robinson, L. F., Annett, A., Badger, M., Jacobel, A. W., Ng, H. C., Opher, J., Pickering, R. A., Taylor, M. L.,  
18 et al.: The biogeochemical impact of glacial meltwater from Southwest Greenland, *Progress in Oceanography*, 176, 102 126, 2019.

19 Holland, D. M., Thomas, R. H., De Young, B., Ribergaard, M. H., and Lyberth, B.: Acceleration of Jakobshavn Isbrae triggered by warm  
20 subsurface ocean waters, *Nature geoscience*, 1, 659–664, 2008.

21 Hopwood, M. J., Connelly, D. P., Arendt, K. E., Juul-Pedersen, T., Stinchcombe, M. C., Meire, L., Esposito, M., and Krishna, R.: Seasonal  
22 changes in Fe along a glaciated Greenlandic fjord, *Frontiers in Earth Science*, 4, 15, 2016.

23 Hyatt, D., Chen, G.-L., LoCascio, P. F., Land, M. L., Larimer, F. W., and Hauser, L. J.: Prodigal: prokaryotic gene recognition and translation  
24 initiation site identification, *BMC bioinformatics*, 11, 1–11, 2010.

25 Jensen, H. M., Pedersen, L., Burneister, A., and Winding Hansen, B.: Pelagic primary production during summer along 65 to 72 N off West  
26 Greenland, *Polar Biology*, 21, 269–278, 1999.

27 Karl, D., Michaels, A., Bergman, B., Capone, D., Carpenter, E., Letelier, R., Lipschultz, F., Paerl, H., Sigman, D., and Stal, L.: Dinitrogen  
28 fixation in the world's oceans, *The nitrogen cycle at regional to global scales*, pp. 47–98, 2002.

29 Knies, J.: Nitrogen isotope evidence for changing Arctic Ocean ventilation regimes during the Cenozoic, *Geophysical Research Letters*, 49,  
30 e2022GL099 512, 2022.

31 Krawczyk, D. W., Yesson, C., Knutz, P., Arboe, N. H., Blicher, M. E., Zinglersen, K. B., and Wagnholt, J. N.: Seafloor habitats across  
32 geological boundaries in Disko Bay, central West Greenland, *Estuarine, Coastal and Shelf Science*, 278, 108 087, 2022.

33 Krupke, A., Mohr, W., LaRoche, J., Fuchs, B. M., Amann, R. I., and Kuypers, M. M.: The effect of nutrients on carbon and nitrogen fixation

i4 by the UCYN-A–haptophyte symbiosis, *The ISME journal*, 9, 1635–1647, 2015.  
i5 Laso Perez, R., Rivas Santisteban, J., Fernandez-Gonzalez, N., Mundy, C. J., Tamames, J., and Pedros-Alio, C.: Nitrogen cycling during an  
i6 Arctic bloom: from chemolithotrophy to nitrogen assimilation, *bioRxiv*, pp. 2024–02, 2024.  
i7 Lewis, K., Van Dijken, G., and Arrigo, K. R.: Changes in phytoplankton concentration now drive increased Arctic Ocean primary production,  
i8 *Science*, 369, 198–202, 2020.  
i9 Li, D., Liu, C.-M., Luo, R., Sadakane, K., and Lam, T.-W.: MEGAHIT: an ultra-fast single-node solution for large and complex metagenomics  
i0 assembly via succinct de Bruijn graph, *Bioinformatics*, 31, 1674–1676, 2015.  
i1 Löscher, C. R., Bourbonnais, A., Dekaezemacker, J., Charoenpong, C. N., Altabet, M. A., Bange, H. W., Czeschel, R., Hoffmann, C., and  
i2 Schmitz, R.: N<sub>2</sub> fixation in eddies of the eastern tropical South Pacific Ocean, *Biogeosciences*, 13, 2889–2899, 2016.  
i3 Löscher, C. R., Mohr, W., Bange, H. W., and Canfield, D. E.: No nitrogen fixation in the Bay of Bengal?, *Biogeosciences*, 17, 851–864, 2020.  
i4 Luo, Y.-W., Doney, S., Anderson, L., Benavides, M., Berman-Frank, I., Bode, A., Bonnet, S., Boström, K. H., Böttjer, D., Capone, D., et al.:  
i5 Database of diazotroph in global ocean: abundance, biomass and nitrogen fixation rates, *Earth System Science Data*, 4, 47–73, 2012.  
i6 Martínez-Pérez, C., Mohr, W., Löscher, C. R., Dekaezemacker, J., Littmann, S., Yilmaz, P., Lehnen, N., Fuchs, B. M., Lavik, G., Schmitz,  
i7 R. A., et al.: The small unicellular diazotrophic symbiont, UCYN-A, is a key player in the marine nitrogen cycle, *Nature Microbiology*, 1,  
i8 1–7, 2016.  
i9 Mills, M. M., Turk-Kubo, K. A., van Dijken, G. L., Henke, B. A., Harding, K., Wilson, S. T., Arrigo, K. R., and Zehr, J. P.: Unusual marine  
i0 cyanobacteria/haptophyte symbiosis relies on N<sub>2</sub> fixation even in N-rich environments, *The ISME Journal*, 14, 2395–2406, 2020.  
i1 Mohr, W., Grosskopf, T., Wallace, D. W., and LaRoche, J.: Methodological underestimation of oceanic nitrogen fixation rates, *PloS one*, 5,  
i2 e12 583, 2010.  
i3 Montoya, J. P.: Nitrogen stable isotopes in marine environments, *Nitrogen in the marine environment*, 2, 1277–1302, 2008.  
i4 Montoya, J. P., Carpenter, E. J., and Capone, D. G.: Nitrogen fixation and nitrogen isotope abundances in zooplankton of the oligotrophic  
i5 North Atlantic, *Limnology and Oceanography*, 47, 1617–1628, 2002.  
i6 Mortensen, J., Rysgaard, S., Winding, M., Juul-Pedersen, T., Arendt, K., Lund, H., Stuart-Lee, A., and Meire, L.: Multidecadal water mass  
i7 dynamics on the West Greenland Shelf, *Journal of Geophysical Research: Oceans*, 127, e2022JC018 724, 2022.  
i8 Munk, P., Nielsen, T. G., and Hansen, B. W.: Horizontal and vertical dynamics of zooplankton and larval fish communities during mid-  
i9 summer in Disko Bay, West Greenland, *Journal of Plankton Research*, 37, 554–570, 2015.  
i0 Murphy, J. and Riley, J. P.: A modified single solution method for the determination of phosphate in natural waters, *Analytica chimica acta*,  
i1 27, 31–36, 1962.  
i2 Myers, P. G. and Ribergaard, M. H.: Warming of the polar water layer in Disko Bay and potential impact on Jakobshavn Isbrae, *Journal of  
i3 Physical Oceanography*, 43, 2629–2640, 2013.  
i4 Patro, R., Duggal, G., Love, M. I., Irizarry, R. A., and Kingsford, C.: Salmon provides fast and bias-aware quantification of transcript  
i5 expression, *Nature methods*, 14, 417–419, 2017.  
i6 Redfield, A. C.: *On the proportions of organic derivatives in sea water and their relation to the composition of plankton (Vol. 1)*. Liverpool:  
i7 university press of liverpool, 1934.  
i8 Reeder, C. F., Stoltenberg, I., Javidpour, J., and Löscher, C. R.: Salinity as a key control on the diazotrophic community composition in the  
i9 Baltic Sea, *Ocean Science Discussions*, 2021, 1–30, 2021.  
i0 Rees, A. P., Gilbert, J. A., and Kelly-Gerreyn, B. A.: Nitrogen fixation in the western English Channel (NE Atlantic ocean), *Marine Ecology*

Formatted: Font: Not Italic

Formatted: Indent: Left: 0 cm, First line: 0 cm

Formatted

11 Progress Series, 374, 7–12, 2009.

12 Robicheau, B. M., Tolman, J., Rose, S., Desai, D., and LaRoche, J.: Marine nitrogen-fixers in the Canadian Arctic Gateway are dominated  
13 by biogeographically distinct noncyanobacterial communities. *FFMS Microbiology Ecology*, 99(12), 122, 2023.

14 Rysgaard, S., Boone, W., Carlson, D., Sejr, M., Bendtsen, J., Juul-Pedersen, T., Lund, H., Meire, L., and Mortensen, J.: An updated view on  
15 water masses on the pan-west Greenland continental shelf and their link to proglacial fjords, *Journal of Geophysical Research: Oceans*,  
16 125, e2019JC015 564, 2020.

17 Schiøtt, S.: The Marine Ecosystem of Ilulissat Icefjord, Greenland, Ph.D. thesis, Department of Biology, Aarhus University, Denmark, 2023.

18 Schlitzer, R.: Ocean data view, 2022.

19 Schvarcz, C. R., Wilson, S. T., Caffin, M., Stancheva, R., Li, Q., Turk-Kubo, K. A., White, A. E., Karl, D. M., Zehr, J. P., and Steward, G. F.:  
20 Overlooked and widespread pennate diatom-diazotroph symbioses in the sea, *Nature communications*, 13, 799, 2022.

21 Shao, Z., Xu, Y., Wang, H., Luo, W., Wang, L., Huang, Y., Agawin, N. S. R., Ahmed, A., Benavides, M., Bentzon-Tilia, M., et al.: Global  
22 oceanic diazotroph database version 2 and elevated estimate of global N 2 fixation, *Earth System Science Data*, 15, 2023.

23 Sherwood, O. A., Davin, S. H., Lehmann, N., Buchwald, C., Edinger, E. N., Lehmann, M. F., and Kienast, M.: Stable isotope ratios in  
24 seawater nitrate reflect the influence of Pacific water along the northwest Atlantic margin, *Biogeosciences*, 18, 4491–4510, 2021.

25 Shiozaki, T., Bombar, D., Riemann, L., Hashihama, F., Takeda, S., Yamaguchi, T., Ehama, M., Hamasaki, K., and Furuya, K.: Basin scale  
26 variability of active diazotrophs and nitrogen fixation in the North Pacific, from the tropics to the subarctic Bering Sea, *Global Biogeochemical Cycles*, 31, 996–1009, 2017.

27 Shiozaki, T., Fujiwara, A., Ijichi, M., Harada, N., Nishino, S., Nishi, S., Nagata, T., and Hamasaki, K.: Diazotroph community structure and  
28 the role of nitrogen fixation in the nitrogen cycle in the Chukchi Sea (western Arctic Ocean), *Limnology and Oceanography*, 63, 2191–  
2205, 2018.

29 Shiozaki, T., Fujiwara, A., Inomura, K., Hirose, Y., Hashihama, F., and Harada, N.: Biological nitrogen fixation detected under Antarctic sea  
30 ice, *Nature geoscience*, 13, 729–732, 2020.

31 Shiozaki, T., Nishimura, Y., Yoshizawa, S., Takami, H., Hamasaki, K., Fujiwara, A., Nishino, S., and Harada, N.: Distribution and survival  
32 strategies of endemic and cosmopolitan diazotrophs in the Arctic Ocean, *The ISME journal*, 17, 1340–1350, 2023.

33 Sigman, D. M., DiFiore, P. J., Hain, M. P., Deutsch, C., Wang, Y., Karl, D. M., Knapp, A. N., Lehmann, M. F., and Pantoja, S.: The dual  
34 isotopes of deep nitrate as a constraint on the cycle and budget of oceanic fixed nitrogen, *Deep Sea Research Part I: Oceanographic  
35 Research Papers*, 56, 1419–1439, 2009.

36 Sipler, R. E., Gong, D., Baer, S. E., Sanderson, M. P., Roberts, Q. N., Mulholland, M. R., and Bronk, D. A.: Preliminary estimates of the  
37 contribution of Arctic nitrogen fixation to the global nitrogen budget, *Limnology and Oceanography Letters*, 2, 159–166, 2017.

38 Slawyk, G., Collos, Y., and Auclair, J.-C.: The use of the 13C and 15N isotopes for the simultaneous measurement of carbon and nitrogen  
39 turnover rates in marine phytoplankton 1, *Limnology and Oceanography*, 22, 925–932, 1977.

40 Sohm, J. A., Webb, E. A., and Capone, D. G.: Emerging patterns of marine nitrogen fixation, *Nature Reviews Microbiology*, 9, 499–508,  
41 2011.

42 Stern, R. W., & Elser, J. J. *Ecological stoichiometry: the biology of elements from molecules to the biosphere*. In *Ecological stoichiometry*,  
43 Princeton university press, 2017.

44 Tang, W., Wang, S., Fonseca-Batista, D., Dehairs, F., Gifford, S., Gonzalez, A. G., Gallinari, M., Planquette, H., Sarthou, G., and Cassar, N.:  
45 Revisiting the distribution of oceanic N2 fixation and estimating diazotrophic contribution to marine production, *Nature communications*,  
46 7

Formatted: Font: Not Italic

Formatted: Font: Not Italic

Formatted: Font: Not Italic

Formatted: Condensed by 0,1 pt

:8 10, 831, 2019.  
:9 Tremblay, J.-É. and Gagnon, J.: The effects of irradiance and nutrient supply on the productivity of Arctic waters: a perspective on climate  
:0 change, in: Influence of climate change on the changing arctic and sub-arctic conditions, pp. 73–93, Springer, 2009.  
:1 Turk, K. A., Rees, A. P., Zehr, J. P., Pereira, N., Swift, P., Shelley, R., Lohan, M., Woodward, E. M. S., and Gilbert, J.: Nitrogen fixation and  
:2 nitrogenase (nifH) expression in tropical waters of the eastern North Atlantic, *The ISME journal*, 5, 1201–1212, 2011.  
:3 Turk-Kubo, K. A., Frank, I. E., Hogan, M. E., Desnues, A., Bonnet, S., and Zehr, J. P.: Diazotroph community succession during the VAHINE  
:4 mesocosm experiment (New Caledonia lagoon), *Biogeosciences*, 12, 7435–7452, 2015.  
:5 Von Friesen, L. W. and Riemann, L.: Nitrogen fixation in a changing Arctic Ocean: an overlooked source of nitrogen?, *Frontiers in Microbi-  
:6 ology*, 11, 596 426, 2020.  
:7 Wang, S., Bailey, D., Lindsay, K., Moore, J., and Holland, M.: Impact of sea ice on the marine iron cycle and phytoplankton productivity,  
:8 *Biogeosciences*, 11, 4713–4731, 2014.  
:9 Zehr, J. P. and Capone, D. G.: Changing perspectives in marine nitrogen fixation, *Science*, 368, eaay9514, 2020.

Formatted: Condensed by 0,1 pt

**Page 3: [1] Deleted**

**Isabell Schlangen**

**28/03/2025 09:54:00**